

1 Accumulation of rosmarinic acid and behaviour of ROS processing systems in *Melissa officinalis* L.
2 under heat stress

3 Laura Pistelli^{a,b,c}, Mariagrazia Tonelli^{a,b}, Elisa Pellegrini^{a,b,c*}, Lorenzo Cotrozzi^a, Chiara
4 Pucciariello^d, Alice Trivellini^d, Giacomo Lorenzini^{a,b,c}, Cristina Nali^{a,b,c}

5 ^a Department of Agriculture, Food and Environment, University of Pisa, Via del Borghetto 80, Pisa
6 56124, Italy

7 ^b CIRSEC, Centre for Climatic Change Impact, University of Pisa, Via del Borghetto 80, Pisa
8 56124, Italy

9 ^c Nutrafood Research Center, University of Pisa, Via del Borghetto 80, 56124 Pisa, Italy

10 ^d Institute of Life Sciences, Scuola Superiore Sant'Anna, Piazza Martiri della Libertà 33, Pisa
11 56127, Italy

12 **ABSTRACT**

13 Heat stress (HS) due to increased air temperature is a major agricultural problem. On the other
14 hand, short-term HS can represent a natural easy-to-use elicitor of bioactive compounds in plants.
15 Similar elicitations can be induced by biotechnological approaches such as hydroponic cultures.
16 The present study pioneering investigated the capability of using a short-term HS (38°C, 5 h) as a
17 tool to rapidly elicit rosmarinic acid (RA) content in leaves of *Melissa officinalis* L. (a species for
18 which RA is the dominant active phenolic compound) hydroponic cultures, highlighting the cross-
19 talk among antioxidant and signalling molecules involved in the heat acclimation. During HS
20 treatment, we found an elicitation of RA biosynthesis associated with (i) an imbalance in reactive
21 oxygen species (ROS) production and scavenging, (ii) an involvement of reduced ascorbate (AsA)
22 in maintaining a high normal reduced state of cells, (iii) an induction of heat shock proteins (i.e.
23 HSP101-like), and (iv) a stimulation of phytohormones. The RA biosynthesis lasted also during the

recovery, although plants activated cellular processes to partially control ROS production, as confirmed by the increased activity of AsA regenerating enzymes, the accumulation of total carotenoids and the stimulation of total antioxidant capacity. The unchanged values of abscisic acid, ethylene and salicylic and jasmonic acids during the recovery phase also documented a reduced demand for protection. The present study represents a wide-ranging investigation of the potential use of HS (without drought interaction) as a technological application for improving bioactive compound production.

Keywords: high temperature, lemon balm, soilless cultivation, rosmarinic acid, signalling systems, antioxidants, heat shock proteins

1. Introduction

Heat stress (HS) is defined as a condition of high air temperature (HT; i.e. 10-15°C above ambient) for a sufficient time to induce a negative impact on plant development, growth and reproduction (Wahid et al., 2007; ~~Hasanuzzaman et al., 2013~~). Plant species and genotypes have several capabilities to cope with HS, and the response depends on the intensity, duration and rate of temperature increase (Wahid et al., 2007). At very HT such as 10-15°C above the ambient air temperature, severe cellular injury and even cell death occur within minutes, caused by a catastrophic collapse of cellular organization (e.g. protein denaturation/aggregation and increased fluidity of membrane lipids; Schöffl et al., 1999). At moderately HT, injuries or death may occur only after long-term exposure, which could be attributed to reduced cellular function and overall plant fitness (Driedonks et al., 2015).

In the plant-HS interaction, an important role is played by the accumulation of reactive oxygen species (ROS; Mittler, 2006). Usually, ROS production rapidly becomes excessive in plants subjected to HS (Pucciariello et al., 2012; Driedonks et al., 2015; Zhao et al., 2018), causing a cellular damage to membranes, organelles, DNA and denaturation/activation of proteins (Howarth,

2005). To prevent this cell damage and regain redox homeostasis, plants can trigger a heat stress response (HSR) by the hyper-activation of non-enzymatic and/or enzymatic ROS scavenging systems (Apel and Hirt, 2004; Halliwell, 2007; Foyer, 2018). The expression and protein level of genes responsible for ROS scavenging are also induced under HS in several plant species (Panchuk et al., 2002; Qiu et al., 2006; Driedonks et al., 2015), and has been associated to basal heat tolerance (Wahid et al., 2007).

Under HS, similarly to other oxidative stresses, the ROS processing system is not only a simple protection mechanism, but also represents a signal for the modulation of other multiple responses (Berkowitz et al., 2016). Therefore, ROS are thought to be involved in the transduction of intra- and intercellular signals controlling gene expression and activity of anti-stress systems (Singh et al., 2019). Several studies documented that HS together with drought lead to an increase of abscisic acid (ABA) concentration that could regulate the acclimation process through the promotion of heat shock proteins (HSP; Larkindale and Knight, 2002; Liu et al., 2006). Asensi-Fabado et al. (2013) reported that prolonged HS (alone or in combination with water stress) induced the synthesis of ABA, salicylic acid (SA) and α -tocopherol in three *Labiatae* species.

Changing perspective, short-term stress conditions can also represent natural easy-to-use elicitors of bioactive compound production in plants. In the last years, many attentions have been given to enhance the production of plant secondary metabolites that are unique sources of pharmaceuticals, food additives, flavors and industrially important biochemicals (Ramakrishna and Ravishankar, 2011; Trivellini et al., 2016; Thakur et al., 2018). Among elicitors, several chemical or physical tools (i.e. signal compounds and/or abiotic factors) have been used. Recently, Khaleghnezhad et al. (2019) demonstrated that the combination of ABA application and HS treatment positively influences the accumulation of secondary metabolites in *Dracocephalum moldavica*. Biotechnological approaches (i.e. shoots, callus, cell suspension and root cultures; Petersen, 2013; D'Angiolillo et al., 2015) can also be used to trigger an array of defense or stress

73 responses that improve the yield of secondary metabolites (Bertoli et al., 2013; Tonelli et al., 2015;
74 Pellegrini et al., 2018; Mosadegh et al., 2018). Hydroponic cultures represent a good approach to
75 investigate the effects of HS alone on plants, in contrast with many reports conducted with standard
76 soil methods where HS was unavoidably combined with other related abiotic stresses (e.g. drought
77 and salinity, Zandalinas et al. 2018).

78 *Melissa officinalis* L. (lemon balm) is an aromatic plant from the Mediterranean area, widely
79 cultivated worldwide (Szabó et al., 2016). High quantities of secondary metabolites such as
80 phenolic compounds, tannins and flavonoids (contained both in leaves and essential oils) were
81 identified/quantified in *M. officinalis* and represent raw material for pharmaceutical, food, beverage,
82 and cosmetic purposes (Moradkhani al., 2010). Rosmarinic acid (RA), which is constitutively
83 accumulated in field-grown plants as antimicrobial compound and as protection against herbivores
84 (Szabo et al., 1999), is the main phenolic compound found in all organs of *M. officinalis*, with a
85 level of about 6% of the dry weight (DW) in leaves (Petersen and Simmonds, 2003). For these
86 reasons, as well as for its fast growth, *M. officinalis* has been exposed to abiotic stress to stimulate
87 some bioactive compounds (e.g. RA, phenols, flavonoids, etc.). Ozone (O₃) exposure caused an
88 alteration in leaf morphology and metabolism both *in vitro* (Tonelli et al., 2015, D'Angiolillo et al.,
89 2015) and *in vivo* plants (Pellegrini et al., 2013) with an enhanced pattern of phenylpropanoids (e.g.
90 phenols, anthocyanins, tannins, carotenoids and RA).

91 The present study pioneering investigated the capability of using a short-term HS as a tool to
92 rapidly increase RA content in leaves of *M. officinalis* hydroponic cultures, highlighting the cross-
93 talk among antioxidant and signalling molecules involved in the heat acclimation. The soilless
94 cultivation allowed the determination of the heating effect, avoiding the crosstalk with drought
95 stress. It is known that different combinations of stresses seem to influence the transcriptome
96 analyses in *Arabidopsis thaliana*, while it cannot be predicted the response of one single stress
97 factor (Rasmussen et al., 2013). Specifically, the purpose of this study was to answer the following

98 questions: (i) Does HS elicit the biosynthesis of RA in *M. officinalis* hydroponic cultures? (ii) What
99 is the behavior of ROS processing systems carrying the potential RA elicitation? (iii) What is the
100 role of hormonal changes in the *M. officinalis*-HS interaction? We hypothesized that the short-
101 period HS could elicit RA production as part of the heat acclimation consisting of a cross-talk
102 among cellular processes and growth regulators tuned by a partial control of ROS production.

103 **2. Materials and methods**

104 *2.1. Plant material, culture conditions and heat treatment*

105 Four-week-old micropropagated shoots (Tonelli et al., 2015) were transferred to hydroponic
106 cultivation using rockwool plug trays (Grodan® Pro Plug) with Hoagland modified nutrient solution
107 (for further details, see supplementary material). The nutrient solution contained the following
108 concentration of macronutrient and trace elements: NO_3^- 14 mM, NH_4^+ 0.5 mM, P 1.2 mM, K^+ 10
109 mM, Ca_2^+ 4.0 mM, Mg_2^+ 0.75 mM, Na^+ 10-01 mM, SO_4^{2-} 1.97 mM, Fe_2^+ 56 μM , BO_3^- 23.1 μM ,
110 Cu_2^+ 1.0 μM , Zn_2^+ 5.0 μM , Mn_2^+ 10 μM , MoO_4^- 1.0 μM . The electrical conductivity and pH of the
111 nutrient solution were, respectively, 1.55-1.80 dS m^{-1} and 5.5-6 (adjusted with diluted H_2SO_4).
112 Cultures were maintained in a growth chamber at $22 \pm 1^\circ\text{C}$, $60 \pm 5\%$ of relative humidity (RH) and
113 under 16 h photoperiod of provided by cool white fluorescent tubes (Philips TLM 40 W/33RS) with
114 $80 \mu\text{mol m}^{-2} \text{s}^{-1}$ photosynthetic active radiation (PAR).

115 After 14-20 days of hydroponic growing, uniformly sized plantlets were placed in a
116 controlled environment fumigation facility under the same climatic conditions as the growth
117 chamber, and then subjected for 5 h to HT ($38 \pm 1^\circ\text{C}$). Shoot samples were collected at 0, 1, 2, 5
118 and 24 h from the beginning of treatment (FBT), instantly frozen in liquid nitrogen and stored at -
119 80°C until biochemical analyses.

120 *2.2. Rosmarinic acid content*

121 Rosmarinic acid content was determined following Tonelli et al. (2015). High performance liquid
122 chromatography (HPLC) separations were performed using a PU-2089 four-solvent low-pressure
123 gradient pump with a UV-2077 UV/Vis multichannel detector (Jasco, Easton, MD, USA). Analyses
124 were performed using a Macherey-Nagel C18 250/4.6 Nucleosil 100-5 column, at a flow rate of 1
125 ml min⁻¹, equipped with a guard column, using acetonitrile (eluent A) and aqueous 0.1% H₃PO₄
126 (eluent B). Rosmarinic acid was detected at 325 nm and quantified on the basis of the integrated
127 peak area, as compared with a standard curve. Further details are reported in supplementary
128 materials.

129 *2.3. ROS production, SOD, CAT and POD activity, lipid peroxidation and antioxidant capacity*

130 Hydrogen peroxide production was estimated fluorimetrically using the Amplex Red Hydrogen
131 Peroxide/Peroxidase Assay Kit (Molecular Probes, Invitrogen, Carlsbad, CA, USA), according to
132 Shin et al. (2005). Spectrofluorimetric determinations were performed with a
133 fluorescence/absorbance microplate reader (Victor3 1420 Multilabel Counter, Perkin Elmer,
134 Waltham, MA, USA) at 530 and 590 nm (excitation and emission resofurin fluorescence,
135 respectively). The superoxide radical (O₂^{•-}) concentration was measured according to Tonelli et al.
136 (2015), after extraction with K/P buffer (50 mM, pH 7.8), with a spectrophotometer (Jenway 6505
137 UV-vis, Cole-Parmer, Stone, UK) at 470 nm, after subtracting the background absorbance due to
138 the buffer solution and to the assay reagents.

139 Enzymes were extracted from plantlet material (200 mg fresh weight, FW) with 2 ml of 50
140 mM sodium phosphate (Na/P) buffer (pH 7.0) containing 1.0 mM EDTA, 1.0 mM PMSF and 2.0%
141 insoluble PVPP (w/v), according to Pistelli et al. (2017). Superoxide dismutase (SOD, EC 1.15.1.1)
142 activity was assayed in terms of its ability to inhibit the photoreduction of NBT, according to the
143 method of Beyer and Fridovich (1987). Spectrophotometer determinations were performed at 560
144 nm (Shimadzu UV-1800, Shimadzu Corporation, Milan, Italy). Catalase (CAT, EC 1.11.1.6)
145 activity was assayed according to the method of Aebi (1984), by monitoring the decomposition of

146 H₂O₂ for 1 min at 240 nm. Peroxidase activity was assayed according to the method of Hemeda and
147 Klein (1990) by measuring the decomposition of H₂O₂ for 10 min at 470 nm. Ascorbate peroxidase
148 (APX, EC 1.11.1.11) activity was assayed according to Nakano and Asada (1981), by measuring
149 the oxidation of AsA at 290 nm for 1 min (at 25°C).

150 Lipid peroxidation was determined by the thiobarbituric acid reactive substances (TBARS)
151 method (Heath and Packer, 1968), after extraction with trichloroacetic acid (TCA; 0.1%, w/v). The
152 malondialdehyde (MDA) concentration was determined at 532 nm corrected for nonspecific
153 turbidity by subtracting the absorbance at 600 nm using a spectrophotometer (Jenway 6505 UV-vis,
154 Cole-Parmer, Stone, UK).

155 The antioxidant properties were assessed spectrofluorimetrically by the Oxygen Radical
156 Absorption Capacity (ORAC) and Hydroxyl Radical Antioxidant Capacity (HORAC) assays (Ou et
157 al., 2001; Ou et al., 2002). Spectrofluorimetric determinations were performed with a
158 fluorescence/absorbance microplate reader (excitation/emission=485/527 nm and 485/520,
159 respectively). The final ORAC values were calculated by using a regression equation between the
160 Trolox concentration and the net area under the fluorescein (FL) decay curve. The final HORAC
161 values were calculated using a regression equation between the standard antioxidant concentration
162 and the net area under the curve. Further details about the investigation of ROS production, SOD
163 activity, lipid peroxidation and antioxidant capacity are reported in supplementary materials.

164 *2.4. Cell and membrane damage*

165 For visualization of dead cells, Evans Blue staining was used according to the method of Keogh et
166 al. (1980) with slight modifications. For determination of H₂O₂, fresh plantlet material was stained
167 with DAB using a modification of the procedure described by Thordal-Christensen et al. (1997).
168 Observations were performed under a light microscope (DM 4000 B, Leica, Wetzlar, Germany).
169 Further details are reported in supplementary materials.

170 2.5. Enzymatic scavenging of ROS

171 Monodehydroascorbate reductase (MDHAR, EC 1.6.5.4) activity was assayed according to the
172 method Huang et al. (2008) by measuring the oxidation of NADH for 1 min through the decrease in
173 absorbance at 340 nm. Dehydroascorbate reductase (DHAR, EC 1.8.5.1) activity was assayed by
174 measuring the production of AsA by dehydroascorbic acid (DHA) reduction at 265 nm for 1 min (at
175 25°C), according to the method of Hossain and Asada (1984). Glutathione reductase (EC 1.6.4.2)
176 activity was assayed according to the method of Foyer and Halliwell (1976) by monitoring the
177 oxidation of NADPH by GSSG for 3 min (at 30°C) through the decrease in absorbance at 340 nm.
178 For all assays, proteins were determined according to Bradford (1976), using bovine serum albumin
179 (BSA) as standard. Further details about the investigation of chloroplast and general enzymatic
180 scavenging of ROS are reported in supplementary materials.

181 2.6. Non-enzymatic scavenging of ROS

182 Ascorbate and DHA content were measured spectrophotometrically, according to Kampfenkel et al.
183 (1995), after extraction with TCA (5%, w/v). This assay is based on the reduction of ferric ion
184 (Fe^{3+}) to ferrous ion (Fe^{2+}) with AsA in acid solution followed by formation of the red chelate
185 between Fe^{2+} and 4,7-diphenyl-1,10-phenanthroline (bathophenanthroline) that absorbs at 525 nm.

186 Total and oxidized glutathione (GSSG) content were measured spectrophotometrically,
187 according to Pellegrini et al. (2013), after extraction with TCA (5%, w/v). This assay is based on an
188 enzymatic recycling procedure in which glutathione was sequentially oxidized by 5,50-dithiobis-2-
189 nitrobenzoic acid and reduced by NADPH in the presence of glutathione reductase. All
190 determinations were performed at 412 nm. Oxidized glutathione was determined after removal of
191 reduced glutathione (GSH) from the sample extract by derivatization with 4-vinilpyridine. The
192 amount of GSH was calculated by subtracting the GSSG amount, as GSH equivalents, from the
193 total glutathione amount.

194 Proline (Pro) content was determined following Bates et al. (1973), after extraction with
195 sulfosalicylic acid (3%, v/v). Spectrophotometric determinations were performed at 520 nm, using
196 toluene as a blank.

197 Carotenoids were measured according to Cotrozzi et al. (2017) after extraction with HPLC-
198 grade methanol. HPLC separations were performed at room temperature with a reverse-phase
199 Dionex column (Acclaim 120, C18, 5 μ m particle size, 4.6 mm internal diameter \times 150 mm length).
200 Further details about the investigation of chloroplast and general non-enzymatic scavenging of ROS
201 are reported in supplementary materials.

202 2.7. Hormones and signalling molecules

203 Absciscic acid was determined by an indirect ELISA based on the use of DBPA1 monoclonal
204 antibody, raised against S(+)-ABA, as described by Trivellini et al. (2011). The ELISA was
205 performed following Walker-Simmons (1987), with minor modifications. Absciscic acid was
206 measured after extraction in distilled water (water: tissue ratio = 10:1, v/w) overnight at 4°C and
207 quantified at 415 nm with an absorbance microplate reader (MDL 680, Perkin-Elmer, Waltham,
208 MA, USA).

209 Fifteen min after excision, ET production was measured by enclosing one plantlet in an air-
210 tight container (250 ml). Gas samples (2 ml) were taken from the headspace of containers after 1 h
211 incubation at 22°C. Ethylene concentration in the sample was measured by a gas chromatograph
212 (HP5890, Hewlett-Packard, Ramsey, MN, USA) using a flame ionization detector, a stainless steel
213 column (150 \times 0.4 cm internal diameter packed with Hysep T). Analytical conditions were as
214 follows: injector and transfer line temperature at 70 and 350°C, respectively, and carrier gas
215 nitrogen at a flow rate of 30 ml min⁻¹ (Mensuali Sodi et al., 1992). Quantification was performed
216 against an external standard.

217 Conjugated and free SA were determined according to Zawoznik et al. (2007), with minor
218 modifications. HPLC separation was performed at room temperature with a Dionex column
219 described above. SA was quantified fluorometrically (RF 2000 Fluorescence Detector, Dionex,
220 USA), with excitation at 305 nm and emission at 407 nm and it was eluted using the mobile phase
221 described above. The flow rate was 0.8 ml min⁻¹. Further details are reported in supplementary
222 material.

223 For JA extraction, platelets were added to 3 ml methanol and incubated overnight at 4°C.
224 HPLC separations were performed with the Dionex system and column described above. Analytical
225 conditions were as follows: absorbance at 210 nm, mobile phase containing 0.2% (v/v) acidified
226 water, and the flow rate was 1 ml min⁻¹ (Kramell et al., 1999). Further details are reported in
227 supplementary material.

228 2.8. Immunoblotting of Hsp 101

229 Proteins were fractionated on a NuPAGE 10% Bis-Tris gel. Blotting was performed on a PVDF
230 membrane, using a Trans-Blot Turbo Transfer System (Biorad, Milan, Italy). The chemiluminescent
231 signal was detected Enhanced ChemiLuminescence reagent (LiteAblot TURBO) and Biospectrum
232 Imaging System (UVP, Analytik Jena, Upland, CA). Amido Black staining of total proteins on the
233 PVDF membrane was performed using standard procedure. Proteomic analyses were performed at
234 0, 1, 2, 3, 4, and 5 h FBT. The immunoblotting was performed in duplicate showing similar results.

235 2.9. Statistics

236 Normality of data was preliminarily tested by the Shapiro-Wilk W test. The effects of high
237 temperature and time were tested using two-way analysis of variance (ANOVA) and comparisons
238 among means were determined by the Tukey's HSD post hoc test. Analyses were performed by
239 NCSS 2000 Statistical Analysis Systems Software (Kaysville, UT, USA).

240 3. Results

241 3.1. Rosmarinic acid content

242 High temperature significantly increased rosmarinic acid content starting to 2 h FBT and reaching a
243 high value at 24 h FBT (+59% in comparison to controls; Fig. 1).

244 3.2. ROS production, SOD activity, lipid peroxidation and antioxidant capacity

245 The content of H_2O_2 and $\text{O}_2^{\bullet-}$ significantly increased under HT throughout the whole experiment.
246 Both parameters reached their maximum already at 1 h FBT (about 2- and 4-fold higher than
247 controls, respectively; Fig. 2 A-B). The activities of SOD, CAT and POD significantly increased
248 under HT already at 1 h FBT (about 2-fold higher than controls, respectively; Fig. 2 C-E), and
249 maintained similar increased levels throughout the whole period of the experiment (except for POD
250 activity at 5 h FBT; Fig. 2 E). Membrane integrity was significantly affected by high temperature as
251 confirmed by the MDA concentrations that were always higher in treated shoots than in controls,
252 starting from 1 h FBT (+100%; Fig. 2 F). The ORAC values showed a similar trend than SOD,
253 already increasing at 1 and 2 h FBT, and even more at 5 and 24 h FBT, when reached levels around
254 100% higher than controls (Fig. 2 G). Compared with controls, HORAC of treated plants
255 significantly decreased at 1 h FBT (-63%), did not show differences at 2 and 5 h FBT, and
256 decreased again at 24 h FBT (Fig. 2 H).

257 3.3. Cell and membrane damage

258 Throughout the whole experiment, leaves appeared macroscopically symptomless. However, HT-
259 injuries were already detectable at the microscopic level just after 1 h FBT, as confirmed by the
260 appearance of dead cells (Fig. 3 A-E). Histological staining showed local accumulation of H_2O_2 in
261 HT-treated material at 5 h FBT, evidenced by reddish-brown areas (Fig. 3 F-J).

262 3.4. Enzymatic scavenging of ROS

263 High temperature strongly decreased APX activity already at 1 h FBT (about 2-fold lower than
264 control), as well as at the other times of analysis (Fig. 4 A). Differently to APX activity, MDHAR
265 and DHAR ones increased throughout the whole experiment under HT, except for DHAR activity at
266 5 h FBT. MDHAR activity especially peaked at 1 h FBT (+281%, compared with controls), and
267 again at 24 h FBT (+49%; Fig. 4 B-C). The activity of GR increased under HT only at 5 h FBT
268 (+65%, compared with controls), but resulted lower in treated material than in control at the end of
269 the recovery period (i.e., 24 h FBT, -66%; Fig. 4 D).

270 3.5. *Non-enzymatic scavenging of ROS*

271 High temperature significantly increased AsA/DHA ratio and Pro content: AsA/DHA ratio started
272 to increase at 1 h FBT and peaked at 2 h FBT (about 2-fold higher than controls; Fig. 5 A); Pro
273 started to increase at 2 h FBT and reached its maximum at 5 h FBT (about 3-fold higher than
274 control; Fig. 5 D). Both AsA/DHA ratio and Pro in treated plants came back to control levels at the
275 end of the recovery period (i.e. 24 h FBT). Differently to AsA/DHA and Pro, GSH/GSSG ratio and
276 total carotenoids (Tot Car) decreased under HT at 1 and 2 h FBT (around -15 and -20% for
277 GSH/GSSG and Tot Car, respectively; Fig. 5 B-C). GSH/GSSG in treated plants recovered at the
278 end of the treatment and remained at control levels at 24 h FBT (Fig. 5 B). Tot Car did not recover
279 at the end of the treatment, but markedly increased at 24 h FBT (+19%, Fig. 5 C).

280 3.7. *Hormones and signalling molecules*

281 High temperature significantly increased all the examined hormones and signalling molecules only
282 during the treatment period, although with a different timing among these molecules (Fig. 6).
283 Absciscic acid reached its maximum at 1 h FBT (10-fold higher than control), slightly decreased at 2
284 and 5 h FBT, and reached control levels at 24 h FBT (Fig. 6 A). Ethylene started to increase at 2 h
285 FBT, reached its maximum at 5 h FBT (2-fold higher than control) and dropped to control levels at
286 24 h FBT (Fig. 6 B). Salicylic acid peaked at 1 h FBT (+690%) and dropped later, reaching control

287 levels at 5 and 24 h FBT (Fig. 6 C); JA slightly increased at 1 h FBT, reached its maximum at 2 h
288 FBT (more than 3-fold higher than control), and came back to control values at 5 and 24 h FBT
289 (Fig. 6 D).

290 3.8. Induction of heat shock protein *Hsp101* under high temperature

291 It has been established that HSP101 plays a major role in thermotolerance (Queitsch et al., 2000),
292 preventing deleterious effects of heat at the cellular levels. In this context, the level of Hsp101
293 protein reached a high level between 2 and 4 hours FBT. Subsequently, the *M. officinalis* HSP101-
294 like level decreased (Fig. 7).

295 4. Discussion

296 4.1. Heat stress elicits the biosynthesis of rosmarinic acid in *Melissa officinalis* hydroponic cultures

297 Plant tissue cultures can be considered a convenient and useful experimental system for (i)
298 examining various factors influencing the biosynthesis of desired products and (ii) exploring
299 effective biotechnologies to enhance their production without interference with pathogens and other
300 microbes (Chattopadhyay et al., 2002). They are considered an alternative to the whole plant in
301 relation to their capacity to produce homogeneous quality and quantity of secondary metabolites,
302 independent of seasonal and geographical limitations (Xu et al., 2011). To enhance the yield of
303 high-value secondary metabolites, plant tissue cultures are manipulated using different strategies,
304 such as the use of physical and chemical elicitors (Khan et al., 2018).

305 Among abiotic stress, it is well known that HS induces the biosynthesis of phenolic
306 compounds (e.g. phenylpropanoids and flavonoids) and suppresses their oxidation (Rivero et al.,
307 2001; Wahid et al., 2007). However, few reports have evaluated the impact of HS on individual
308 metabolites (Fletcher et al., 2005; Khaleghnezhad et al., 2019). Here, our study shows a significant
309 increase of RA content in *M. officinalis* hydroponic cultures under HT, from 2 h FBT until the end
310 of the experiment (i.e. 24 h FBT; Figure 1), identifying HT as a RA elicitor. Although Fletcher et al.

311 (2005) reported that prolonged HS (30°C day/night for 4 weeks) negatively regulated RA
312 accumulation by causing a potential rapid biological breakdown of RA in *Mentha spicata* leaves,
313 our outcome is in agreement with a number of previous studies focused on other stressors: the
314 stimulation of RA by biotic (such as yeast elicitor) and abiotic elicitors (e.g. silver ions, methyl
315 jasmonate and O₃) has been previously observed in cell cultures of several plants [e.g.
316 *Lithospermum erythrorhizon* (Ogata et al., 2004), *Coleus blumei* (Petersen et al., 1994; Szabo et al.,
317 1999), and *Salvia miltiorrhiza* (Yan et al., 2006; Zhao et al., 2010)], including *M. officinalis*
318 (Tonelli et al., 2015).

319 4.2. ROS generation and scavenging during rosmarinic acid elicitation

320 One of the events occurring in response to HSs is ROS production (for a review see Suzuki and
321 Mittler, 2006; Suzuki et al., 2014) and oxidative stress is involved directly or indirectly in the RA
322 accumulation observed in our study. Although visible symptoms of oxidative stress were absent in
323 plants subjected to HT, DAB staining and Evan's blue incorporation indicated that H₂O₂ deposition
324 and cell death events occurred starting at 1 h FBT. The loss of membrane integrity was also
325 confirmed by the significant build-up of MDA by-products observed starting at 1 h FBT, revealing
326 that membrane lipid peroxidation occurred (Zhao et al., 2018). Both H₂O₂ and O₂^{•-} contents
327 increased at the same time, confirming that an imbalance in ROS production and scavenging
328 occurred (Demidchik, 2015). To deal with oxidative damage, plants have evolved different ROS
329 processing systems that are able to respond to ROS production and to transmit the stress signals
330 (Foyer, 2018). Chloroplasts contain several pathways that limit H₂O₂ accumulation and maintain
331 cellular redox potential, including the Halliwell-Asada cycle (Foyer and Shigeoka, 2011). In our
332 study, AsA/DHA ratio significantly and quickly increased under HT-treatment (Fig. 5), confirming
333 the involvement of AsA in maintaining a high normal reduced state of cells, as well as in signalling
334 and/or limiting the inhibitory effects of ROS-induced oxidative stress (Meyer, 2008; Pellegrini et
335 al., 2013; Zou et al., 2016). The reduced state of AsA observed under HT treatment might be

336 ascribable to (i) the activity of AsA regenerating enzymes, as confirmed by the increased activity of
337 MDHAR and DHAR during the initial and recovery phases (Fig. 4) and (ii) the capability of
338 converting GSSG in GSH, via the Halliwell-Asada cycle (Gill and Tuteja, 2010). The GSH/GSSG
339 ratio (an indicator of general cellular redox balance) showed a marked decrease during the first two
340 hours of HT treatment (Fig. 5; although GR activity remain unchanged), indicating that GSH plays
341 a role in mediating the defense responses of plant cells to HS (Zou et al., 2016). Concomitantly,
342 SOD, CAT and POD activities increase was observed in HT-treated shoots throughout the whole
343 experiment, suggesting the subsequent reduction of superoxide to water. This response has been
344 already detected in other plants to counteract the ROS production during HS condition (Suzuki et al.
345 2014; Zhao et al., 2018). Indeed, the levels of the oxidative-damage markers (i.e. ROS and MDA
346 contents) decreased at the end of the treatment as well as after recovery, reaching values slightly
347 higher than controls (similarly to SOD activity). These outcomes suggest that *M. officinalis*
348 hydroponic cultures activated cellular processes to partially control ROS production (e.g. ROS
349 contents never reached levels to cause visible symptoms) and to induce a heat acclimation. In this
350 context, the protective function of HSP might occur only under the first hours of HS (i.e. from 2 to
351 4 h FBT), as suggested by the transient induction of HSP101-like in treated plants (Fig. 7). The
352 activation of HSPs plays an essential role in preventing or minimizing the harmful effect of heat at
353 the molecular level (Gullì et al., 2007). A signal cascade for HS response activated by HS
354 Transcription Factors (HSF) has been extensively examined in promoting the transcription of HSP
355 genes in abiotic stress conditions where ROS are produced (Guo et al. 2016). The subsequent heat
356 acclimation included the prolonged RA elicitation that was maintained also during the recovery
357 phase.

358 Among other non-enzymatic processing systems, carotenoids are pigments that play a
359 multitude of functions in plant metabolism including photoprotection, prevention of peroxidative
360 damage to the membrane lipids, and ROS scavenging (Havaux, 1998). In our study, Tot Car content

361 decreased starting from 1 h FBT, but it significantly increased at the recovery time, suggesting that
362 these metabolites could be consumed by the cell to minimize the possible ROS generation and
363 stabilize the lipid phase of the thylakoid membranes (as confirmed by H₂O₂, O₂[•] and MDA levels
364 returned slightly higher than controls after the HT treatment; Sharma et al., 2012).

365 A key adaptive mechanism in many plants grown under abiotic stress is the production of
366 organic compounds of low molecular mass involved in osmotic adjustments (Hare et al., 1998).
367 Proline not only facilitates water uptake, but also protects cells against ROS accumulation under
368 stress conditions by recycling of NADPH via its synthesis from glutamate and acting as a free
369 radical scavenger (Soares et al., 2018). In our study, Pro accumulation was observed at 2 and 5 h
370 FBT, indicating that also this compound likely participated in the reduction of oxidative damage by
371 buffering cellular redox potential (Verbruggen and Hermans, 2008) and enhancing photochemical
372 electron transport activity (Zhao et al., 2018).

373 To further evaluate the ability of ROS processing systems to provide defense and regenerate
374 the active reduced forms, we also analyzed the total antioxidant capacity of *M. officinalis*
375 hydroponic cultures. According to the ORAC assay, the antioxidant capacity was significantly
376 enhanced under HT throughout the entire period of the experiment, confirming the marked free-
377 radical scavenging ability of antioxidants (in particular against peroxy radical) in treated shoots
378 (Pellegrini et al., 2013). According to the HORAC method, instead, the antioxidant capacity
379 initially decreased at 1 h FBT, did not change at 2 and 5 h FBT, and decreased again at the recovery
380 time. This outcome indicates the reduced radical prevention ability of treated shoots (expressed as
381 metal-chelating properties of antioxidants; Ou et al., 2002; Marchica et al., 2019). It is worth to note
382 that ORAC and HORAC assays measure two different, but equally important, aspects of antioxidant
383 properties (radical chain breaking and radical prevention, respectively). Consequently, it is expected
384 that the samples with high ORAC values do not necessarily have high HORAC values, and vice
385 versa (Ou et al. 2002).

386 4.3. Hormonal changes in *M. officinalis* under heat stress.

387 Several studies have documented that HS can induce an alteration of hormonal homeostasis by
388 modifying the biosynthesis and/or the compartmentalization of the main signalling molecules such
389 as ABA, ET, SA and JA (Maestri et al., 2002; Wahid et al. 2007). Absciscic acid is a ubiquitous
390 phytohormone with a key role in the tolerance to stressful conditions that quickly affect plant water
391 balance through the regulation of stomatal closure (Basu and Rabara, 2017). In the present study,
392 the variation of ABA, which severely raised at 1 h FBT and then decreased at 2 and 5 h FBT, and
393 finally reached control levels at the recovery time, confirms the involvement of this phytohormone
394 in biochemical pathways essential for triggering HS-acclimation during the initial phase of *M.*
395 *officinalis* response to HT treatment (Kurepin et al., 2008; Asensi-Fabado et al., 2013). Interesting
396 recent results demonstrated that the combination of HS treatment and exogenous ABA application
397 positively influences the accumulation of RA in dragonhead plants (Khaleghnezhad et al. 2019).
398 Conversely, ET production increased under HT-treatment only at 2 and 5 h FBT, indicating that this
399 gaseous hormone likely took part in consecutive events to regulate HT-tolerance and to protect
400 against HT-induced oxidative stress (Suzuki et al., 2005; Asensi-Fabado et al., 2013). Ethylene, SA
401 and JA are important components of signalling pathways involved in response to abiotic stresses
402 (UV, O₃ and heat; Kohli et al., 2013; Pellegrini et al., 2013, 2016; Cotrozzi et al., 2017; Landi et al.,
403 2019). Salicylic acid has been found to mediate heat tolerance through increases in antioxidant
404 enzyme activities and heat-induced oxidative stress alleviation (Larkindale and Knight, 2002; Pan et
405 al., 2006; Liu et al., 2006). Few studies to date have investigated the implications of JA in heat
406 tolerance; however, some lines of evidence suggest that this compound is involved in the regulation
407 of HS tolerance in *Arabidopsis* (Kazan, 2015). In our study, the concomitant increase of SA and JA
408 levels observed during the first two hours of HT (SA peaked at 1 h FBT, whereas JA peaked at 2 h
409 FBT) confirms that a multifactorial regulation of shoot HT-acclimation occurred (Clarke et al.,
410 2009). Interestingly, the unchanged values of ABA, ET, SA and JA at the recovery time might be

411 related to a reduced demand for protection, suggesting a key role for these hormones in HT-
412 acclimation signalling causing the above-described ROS regulation and RA elicitation (Clarke et
413 al., 2004).

414 In conclusion, our study shows that short-period HT is a valuable tool to improve the
415 production of high-value secondary metabolites in *M. officinalis* shoots. At the timing and level
416 utilized in this study, HT induced a cross-talk between cellular processes and growth regulators
417 which induced a partial control of ROS production, and led to an HT-acclimation involving a
418 RA elicitation, without causing macroscopic damage to the plants. The present study represents a
419 pioneering and wide-ranging investigation of the potential use of HT (without drought interaction)
420 as a technological application for improving bioactive compound production.

421 **Acknowledgments**

422 We gratefully acknowledge Dr. Rita Maggini for the RA determinations. Mr. Andrea Parrini
423 supervised the growth chamber.

424 **Appendix A. Supplementary data**

425 **References**

- 426 Aebi, H., 1984. Catalase *in vitro*. Methods Enzymol. 105, 121-126.
- 427 Apel, K., Hirt, H., 2004. Reactive oxygen species: metabolism, oxidative stress, and signal
428 transduction. Annu. Rev. Plant Biol. 55, 373-393.
- 429 Asensi-Fabado, M.A., Oliván, A., Munné-Bosch, S., 2013. A comparative study of the hormonal
430 response to high temperatures and stress reiteration in three *Labiatae* species. Environ. Exp. Bot.
431 94, 57-65.

432 Basu, S., Rabara, R., 2017. Absciscic acid - an enigma in the abiotic stress tolerance of crop plants.
 433 Plant Gene 11, 90-98.

434 Bates, L.S., Waldren, R.P., Teare, I.D., 1973. Rapid determination of free proline for water-stress
 435 studies. Plant Soil 39, 205-207.

436 Berkowitz, O., De Clercq, I., Van Breusegem, F., Whelan, J., 2016. Interaction between hormonal
 437 and mitochondrial signaling during growth, development and in plant defence responses. Plant Cell
 438 Environ. 39, 1127-1139.

439 Bertoli, A., Lucchesini, M., Mensuali-Sodi, A., Leonardi, M., Doveri, S., Magnabosco, L., Pistelli,
 440 L., 2013. Aroma characterization and UV elicitation of purple basil from different plant tissue
 441 cultures. Food Chem. 141, 776-787.

442 Beyer, W.F., Fridovich, I., 1987. Assaying for superoxide dismutase activity: some large
 443 consequences of minor changes in conditions. Anal. Biochem. 161, 559-566.

444 Bradford, M.M., 1976. A rapid and sensitive method for the quantitation of microgram quantities of
 445 protein utilizing the principle of protein-dye binding. Anal. Biochem. 7, 248-254.

446 Chattopadhyay, S., Farkya, S., Srivastava, A.K., Bisaria, V.S., 2002. Bioprocess considerations for
 447 production of secondary metabolites by plant cell suspension cultures. Biotechnol. Bioprocess Eng.
 448 7, 138-149.

449 Clarke, S.M., Cristescu, S.M., Miersch, O., Harren, F.J.M., Wasternack, C., Mur, L.A.J., 2009.
 450 Jasmonates act with salicylic acid to confer basal thermotolerance in *Arabidopsis thaliana*. New
 451 Phytol. 182, 172-187.

452 Clarke, S.M., Mur, L.A.J., Wood, J.E., Scott, I.M., 2004. Salicylic acid dependent signaling
 453 promotes basal thermotolerance but is not essential for acquired thermotolerance in *Arabidopsis*
 454 *thaliana*. The Plant J. 38, 432-447.

455 Cotrozzi, L., Pellegrini, E., Guidi, L., Landi, M., Lorenzini, G., Massai, R., Remorini, D., Tonelli,
 456 M., Trivellini, A., Vernieri, P., Nali, C., 2017. Losing the warning signal: drought compromises the
 457 cross-talk of signaling molecules in *Quercus ilex* exposed to ozone. Front. Plant Sci. 8, doi:
 458 10.3389/fpls.2017.01020.

459 D'Angiolillo, F., Tonelli, M., Pellegrini, E., Nali, C., Lorenzini, G., Pistelli, L., Pistelli, L., 2015.
 460 Can ozone alter the terpenoid composition and membrane integrity of *in vitro* *Melissa officinalis*
 461 shoots? Nat. Prod. Commun. 10, 1055-1058.

462 Demidchik, V., 2015. Mechanisms of oxidative stress in plants: from classical chemistry to cell
 463 biology. Environ. Exp. Bot. 109, 212-228.

464 Driedonks, N., Xu, J., Peters, J.L., Park, S., Rieu, I., 2015. Multi-level interactions between heat
 465 shock factors, heat shock proteins, and the redox system regulated acclimation to heat. Front. Plant
 466 Sci. 6, 999 doi: 10.3389/fpls.2015.00999.

467 Fletcher, R.S., Slimmon, T., McAuley, C.Y., Kott, L.S., 2005. Heat stress reduces the accumulation
 468 of rosmarinic acid and the total antioxidant capacity in spearmint (*Mentha spicata* L.). J. Sci. Food
 469 Agric. 85, 2429-2436.

470 Foyer, C.H., 2018. Reactive oxygen species, oxidative signaling and the regulation of
 471 photosynthesis. Environ. Exp. Bot. 154, 134-142.

472 Foyer, C.H., Halliwell, B., 1976. The presence of glutathione and glutathione reductase in
 473 chloroplast: a proposed role in ascorbic acid metabolism. Planta 133, 21-25.

474 Foyer, C.H., Shigeoka, S., 2011. Understanding oxidative stress and antioxidant functions to
 475 enhance photosynthesis. Plant Physiol. 155, 93-100.

476 Gill, S.S., Tuteja, N., 2010. Reactive oxygen species and antioxidant machinery in abiotic stress
 477 tolerance in crop plants. Plant Physiol. Biochem. 48, 909-930.

478 Gullì, M., Corradi, M., Rampino, P., Marmioli, N., Perrotta, C., 2007. Four members of the
 479 HSP101 gene family are differently regulated in *Triticum durum* Desf. FEBS letters 581, 4841-
 480 4849.

481 Guo, M., Liu, J. H., Ma, X., Luo, D. X., Gong, Z.H., Lu, M.H., 2016. The plant heat stress
 482 transcription factors (HSFs): structure, regulation, and function in response to abiotic stresses.
 483 Front. Plant Sci. 7, 114, doi: 10.3389/fpls.2016.00114.

484 Halliwell, B., 2007. Biochemistry of oxidative stress. Bioch. Soc. Trans. 35, 1147-1150.

485 Hare, P.D., Cress, W.A., Staden, J.V., 1998. Dissecting the roles of osmolyte accumulation during
 486 stress. Plant Cell Environ. 21, 535-553.

487 Havaux, M., 1998. Carotenoids as membrane stabilizers in chloroplasts. Trends Plant Sci. 3, 147-
 488 151.

489 Heath, R.L., Packer, L., 1968. Photoperoxidation in isolated chloroplasts. I. Kinetics and
 490 stoichiometry of fatty acid peroxidation. Arch. Biochem. Biophys. 125, 180-198.

491 Hemeda, H.M., Klein B.P., 1990. Effects of naturally occurring antioxidants on peroxidase activity
 492 of vegetable extracts. J. Food Sci. 55, 184-185.

493 Hossain, M.A., Asada, K., 1984. Purification of dehydroascorbate reductase from spinach and its
 494 characterization as a thiol enzyme. Plant Cell Physiol. 25, 85-92.

495 Howarth, C.J., 2005. Genetic improvements of tolerance to high temperature. In Ashraf, M., Harris,
 496 P.J.C. (Eds.), Abiotic stresses: plant resistance through breeding and molecular approaches.
 497 Howarth Press Inc., New York.

498 Huang, G.J., Lai, H.C., Chang, Y.S., Sheu, M.J., Lu, T.L., Huang, S.S., Lin, Y.H., 2008.
 499 Antimicrobial, dehydroascorbate reductase, and monodehydroascorbate reductase activities of

500 defensin from sweet potato [*Ipomoea batatas* (L.) Lam. "Tainong 57"] storage roots. J. Agric. Food
501 Chem. 56, 2989-2995.

502 Kampfenkel, K., Van Montagu, M., Inzé, D., 1995. Extraction and determination of ascorbate and
503 dehydroascorbate from plant tissue. Anal. Biochem. 10, 165-167.

504 Kazan, K., 2015. Diverse roles of jasmonates and ethylene in abiotic stress tolerance. Trends Plant
505 Sci. 20, 219-229.

506 Khaleghnezhad, V., Yousefi, A.R., Tavakoli, A., Farajmand, B., 2019. Interactive effects of abscisic
507 acid and temperature on rosmarinic acid, total phenolic compounds, anthocyanin, carotenoid and
508 flavonoid content of dragonhead (*Dracocephalum moldavica* L.). Sci. Hortic. 250, 302-309.

509 Khan, T., Abbasi, B.H., Khan, M.A., 2018. The interplay between light, plant growth regulators and
510 elicitors on growth and secondary metabolism in cell cultures of *Fagonia indica*. J. Photochem.
511 Photobiol. 185, 153-160.

512 Keogh, R.C., Deverall, B.J., McLeod, S., 1980. Comparison of histological and physiological
513 responses to *Phakopsora pachyrhizi* in resistant and susceptible soybean. Trans. Br. Mycol. Soc. 74,
514 329-333.

515 Kohli, A., Sreenivasulu, N., Lakshmanan, P., Kumar, P.P., 2013. The phytohormones crosstalk
516 paradigm takes center stage in understanding how plants respond to abiotic stress. Plant Cell Rep.
517 32, 945-957.

518 Kramell, R., Miersch, O., Schneider, G., Wasternack, C., 1999. Liquid chromatography of jasmonic
519 acid amine conjugates. Chromatographia 49, 42-46.

520 Kurepin, L.V., Qaderi, M.M., Back, T.G., Reid, D.M., Pharis, R.P., 2008. A rapid effect of applied
521 brassinolide on abscisic acid concentrations in *Brassica napus* leaf tissue subjected to short-term
522 heat stress. Plant Growth Reg. 55, 165-167.

523 Landi, M., Crottozzi, L., Pellegrini, E., Remorini, D., Tonelli, M., Trivellini, A., Nali, C., Guidi, L.,
 524 Massai, R., Vernieri, P., Lorenzini, G., 2019. When “thirsty” means “less able to activate the
 525 signalling wave triggered by a pulse of ozone”: a case of study in two Mediterranean deciduous oak
 526 species with different drought sensitivity. *Sci. Tot. Environ.* 657, 379-390.

527 Larkindale, J., Knight, M.R., 2002. Protection against heat stress-induced oxidative damage in
 528 *Arabidopsis* involves calcium, abscisic acid, ethylene, and salicylic acid. *Plant Physiol.* 128, 682-
 529 695.

530 Liu, H.T., Liu, Y.Y., Pan, Q.H., Yang, H.R., Zhan, J.C., Huang, W.D., 2006. Novel
 531 interrelationship between salicylic acid, abscisic acid, and PIP₂-specific phospholipase C in heat
 532 acclimation-induced thermotolerance in pea leaves. *J. Exp. Bot.* 57, 3337-3347.

533 Maestri, E., Klueva, N., Perrotta, C., Gulli, M., Nguyen, H.T., Marmiroli, N., 2002. Molecular
 534 genetics of heat tolerance and heat shock proteins in cereals. *Plant Mol. Biol.* 48, 667-681.

535 Marchica, A., Lorenzini, G., Papini, R., Bernardi, R., Nali, C., Pellegrini, E., 2019. Signalling
 536 molecules responsive to ozone-induced oxidative stress in *Salvia officinalis*. *Sci. Tot. Environ.* 657,
 537 568-576.

538 Mensuali Sodi, A., Panizza, M., Tognoni, F., 1992. Quantification of ethylene losses in different
 539 container-seal system and comparison of biotic and abiotic contributions to ethylene accumulation
 540 in cultured tissues. *Physiol. Plant.* 84, 472-476.

541 Meyer, A.J., 2008. The integration of glutathione homeostasis and redox signalling. *J. Plant*
 542 *Physiol.* 165, 1390-1403.

543 Mittler, R., 2006. Abiotic stress, the field environment and stress combination. *Trends Plant Sci.* 11,
 544 15-19.

545 Moradkhani, H., Sargsyan, E., Bibak, H., Naseri, B., Sadat-Hosseini, M., Fayazi-Barjin, A.,
 546 Meftahizade, H., 2010. *Melissa officinalis* L., a valuable medicine plant: a review. J. Med. Plant
 547 Res. 4, 2753-2759.

548 Mosadegh, H., Trivellini, A., Ferrante, A., Lucchesini, M., Vernieri, P., Mensuali, A., 2018.
 549 Applications of UV-B lighting to enhance phenolic accumulation of sweet basil. Sci. Hortic. 229,
 550 107-116.

551 Murashige, T., Skoog, F., 1962. A revised medium for rapid growth and bioassays with tobacco
 552 tissue cultures. Physiol. Plant. 15, 473-497.

553 Nakano, Y., Asada, K., 1981. Hydrogen peroxide is scavenged by ascorbate-specific peroxidase in
 554 spinach chloroplasts. Plant Cell Physiol. 22, 867-880.

555 Ogata, A., Tsuruga, A., Matsuno, M., Mizukami, H., 2004. Elicitor induced rosmarinic acid
 556 biosynthesis in *Lithospermum erythrorhizon* cell suspension cultures: activities of rosmarinic acid
 557 synthase and the final two cytochrome P450-catalyzed hydroxylations. Plant Biotechnol. 21, 393-
 558 396.

559 Ou, B.X., Hampsch-Woodill, M., Prior, R.L., 2001. Development and validation of an improved
 560 Oxygen Radical Absorbance Capacity Assay using fluorescein as the fluorescent probe. J. Agric.
 561 Food Chem. 49, 4619-4626.

562 Ou, B.X., Huang, D.J., Hampsch-Woodill, M., Flanagan, J.A., Deemer, E.K., 2002. Analysis of
 563 antioxidant activities of common vegetables employing oxygen radical absorbance capacity
 564 (ORAC) and ferric reducing antioxidant power (FRAP) assays: a comparative study. J. Agric. Food
 565 Chem. 50, 3122-3128.

566 Pan, Q., Zhan, J., Liu, H., Zhang, J., Chen, J., Wen, P., Huang, W., 2006. Salicylic acid synthesized
 567 by benzoic acid 2-hydroxylase participates in the development of thermotolerance in pea plants.
 568 Plant Sci. 171, 226-233.

569 Panchuk, I.I., Volkov, R.A., Schöffl, F., 2002. Heat stress-and heat shock transcription factor-
 570 dependent expression and activity of ascorbate peroxidase in *Arabidopsis*. Plant Physiol. 129, 838-
 571 853.

572 Pellegrini, E., Campanella, A., Crottozzi, L., Tonelli, M., Nali, C., Lorenzini, G., 2018. Ozone
 573 primes changes in phytochemical parameters in the medicinal herb *Hypericum perforatum* (St.
 574 John's wort). Ind. Crops Prod. 126, 119-128.

575 Pellegrini, E., Trivellini, A., Campanella, A., Francini, A., Lorenzini, G., Nali, C., Vernieri, P.,
 576 2013. Signaling molecules and cell death in *Melissa officinalis* plants exposed to ozone. Plant Cell
 577 Rep. 32, 1965-1980.

578 Pellegrini, E., Trivellini A., Crottozzi L., Vernieri P., Nali C., 2016. Involvement of phytohormones
 579 in plant responses to ozone. In Ahammed, G.J., Yu, J.-Q. (Eds.), Plant hormones under challenging
 580 environmental factors. Springer Science, Dordrecht, pp. 215-245.

581 Petersen, M., 2013. Rosmarinic acid: new aspects. Phytochem. Rev. 12, 207-227.

582 Petersen, M., Häusler, E., Meinhard, J., Karwatzki, B., Gertlowski, C., 1994. The biosynthesis of
 583 rosmarinic acid in suspension cultures of *Coleus blumei*. Plant Cell Tissue Organ Cult. 38, 171-179.

584 Petersen, M., Simmonds, M.S.J., 2003. Molecules of interest: rosmarinic acid. Phytochemistry, 62,
 585 121-125.

586 Pistelli, L., D'Angiolillo, F., Morelli, E., Basso, B., Rosellini, I., Posarelli, M., Barbieri, M., 2017.
 587 Response of spontaneous plants from an ex-mining site of Elba island (Tuscany, Italy) to
 588 metal(loid) contamination. Environ. Sci. Pollut. Res. 24, 7809-7820.

589 Pucciariello, C., Banti, V., Perata, P., 2012. ROS signaling as common element in low oxygen and
590 heat stresses. *Plant Physiol. Biochem.* 59, 3-10.

591 Qiu, X.-B., Shao, Y.-M., Miao, S., Wang, L., 2006. The diversity of the DnaJ/Hsp40 family, the
592 crucial partners for Hsp70 chaperones. *Cell. Mol. Life Sci.* 63, 2560-2570.

593 Queitsch, C., Hong, S. W., Vierling, E., Lindquist, S., 2000. Heat shock protein 101 plays a crucial
594 role in thermotolerance in *Arabidopsis*. *The Plant Cell* 12, 479-492.

595 Ramakrishna, A., Ravishankar, G.A., 2011. Influence of abiotic stress signals on secondary
596 metabolites in plants. *Plant Signal. Behav.* 6, 1720-1731.

597 Rasmussen, S., Barah, P., Suarez-Rodriguez, M. C., Bressendorff, S., Friis, P., Costantino, P.,
598 Bones, A.M., Nielsen, H.B., Mundy, J., 2013. Transcriptome responses to combinations of stresses
599 in *Arabidopsis*. *Plant Physiol.* 161, 1783-1794.

600 Rivero, R.M., Ruiz, J.M., Garcia, P.C., Lopez-Lefebvre, L.R., Sanchez, E., Romero, L., 2001.
601 Resistance to cold and heat stress: accumulation of phenolic compounds in tomato and watermelon
602 plants. *Plant Sci.* 160, 315-321.

603 Schöffl, F., Prandl, R., Reindl, A., 1999. Molecular response to heat stress. In: Shinozaki, K.,
604 Yamaguchi-Shinozaki, K., (Eds.), *Molecular responses to cold, drought, heat and salt stress in*
605 *higher plants*. R.G. Landes Co., Austin, Texas, pp. 81-89.

606 Sharma, P., Jha, A.B., Dubey, R.S., Pessarakli, M., 2012. Reactive oxygen species, oxidative
607 damage, and antioxidative defense mechanisms in plants under stressful conditions. *J. Bot.* 217037
608 doi:10.1155/2012/217037.

609 Shin, R., Berg, R.H., Schachtman, D.P., 2005. Reactive oxygen species and root hairs in
610 *Arabidopsis* root response to nitrogen, phosphorus and potassium deficiency. *Plant Cell Physiol.* 46,
611 1350-1357.

612 Singh, A., Kumar, A., Yadav, S., Singh, I.K., 2019. Reactive oxygen species-mediated signaling
 613 during abiotic stress. *Plant Gene* 18, 100173- doi.org/10.1016/j.plgene.2019.100173.

614 Soares, C., Carvalho, M.E.A., Azevedo, R.A., Fidalgo, F., 2018. Plants facing oxidative challenges
 615 - a little help from the antioxidant networks. *Environ. Exp. Bot.*
 616 doi.org/10.1016/j.envexpbot.2018.12.009.

617 Suzuki, N., Mittler, R., 2006. Reactive Oxygen Species and temperature stresses: a delicate balance
 618 between signaling and destruction. *Physiol. Plant.* 126, 45-51.

619 Suzuki, N., Rivero, R.M., Shulaev, V., Blumwald, E., Mittler, R., 2014. Abiotic and biotic stress
 620 combinations. *New Phytol.* 203, 32-43.

621 Suzuki, N., Rizhsky, L., Liang, H., Shuman, J., Shulaev, V., Mittler, R., 2005. Enhanced tolerance
 622 to environmental stress in transgenic plants expressing the transcriptional coactivator multiprotein
 623 bridging factor 1c. *Plant Physiol.* 139, 1313-1322.

624 Szabo, E., Thelen, A., Petersen, M., 1999. Fungal elicitor preparations and methyl jasmonate
 625 enhance rosmarinic acid accumulation in suspension cultures of *Coleus blumei*. *Plant Cell Rep.* 18,
 626 485-489.

627 Szabó, K., Malekzadeh, M., Radácsi, P., Ladányi, M., Rajhárt, P., Inotai, K., Tavaszi-Sárosi,
 628 Németh, É., 2016. Could the variety influence the quantitative and qualitative outcome of lemon
 629 balm production? *Ind. Crops Prod.* 83, 710-716.

630 Thakur, M., Bhattacharya, S., Khosla, P.K., Puri, S., 2018. Improving production of plant secondary
 631 metabolites through biotic and abiotic elicitation. *J. Appl. Res. Med. Aromat. Plants*
 632 doi.org/10.1016/j.jarmap.2018.11.004.

633 Thordal-Christensen, H., Zhang, Z., Wei, Y., Collinge, D.B., 1997. Subcellular localization of H₂O₂
634 in plants. H₂O₂ accumulation in papillae and hypersensitive response during the barley-powdery
635 mildew interaction. *Plant J.* 11, 1187-1194.

636 Tonelli, M., Pellegrini, E., D'Angiolillo, F., Petersen, M., Nali, C., Pistelli, L., Lorenzini, G., 2015.
637 Ozone-elicited secondary metabolites in shoot cultures of *Melissa officinalis* L. *Plant Cell Tissue*
638 *Org. Cult.* 120, 617-629.

639 Trivellini, A., Ferrante, A., Vernieri, P., Serra, G., 2011. Effects of abscisic acid on ethylene
640 biosynthesis and perception in *Hibiscus rosa-sinensis* L. flower development. *J. Exp. Bot.* 62, 5437-
641 5452.

642 Trivellini, A., Lucchesini, M., Maggini, M., Mosadegh, H., Sulca Villamarin, T.S., Vernieri, P.,
643 Mensuali, A., Pardossi A., 2016. Lamiaceae phenols as multifaceted compounds: bioactivity,
644 industrial prospects and role of “positive-stress”. *Ind. Crops Prod.* 83, 241–254.

645 Verbruggen, N., Hermans, C., 2008. Proline accumulation in plants: a review. *Amino Acids* 35,
646 753-759.

647 Wahid, A., Gelani, S., Ashraf, M., Foolad, M.R., 2007. Heat tolerance in plants: an overview.
648 *Environ. Exp. Bot.* 61, 199-223.

649 Walker-Simmons, M. 1987. ABA levels and sensitivity in developing wheat embryos of sprouting
650 resistant and susceptible cultivars. *Plant Physiol.* 84, 61-66.

651 Xu, J., Ge, X., Dolan, M.C., 2011. Towards high-yield production of pharmaceutical proteins with
652 plant cell suspension cultures. *Biotechnol. Adv.* 29, 278-299.

653 Yan, Q., Shi, M., Ng, J., Wu, J.Y., 2006. Elicitor-induced rosmarinic acid accumulation and
654 secondary metabolism enzyme activities in *Salvia miltiorrhiza* hairy roots. *Plant Sci.* 170, 853-858.

655 Zandalinas, S.I., Mittler, R., Balfagón, D., Arbona, V., Gómez-Cadenas, A., 2018. Plant adaptations
656 to the combination of drought and high temperatures. *Physiol. Plant.* 162, 2-12.

657 Zawoznik, M., Groppa, M.D., Tomaro, M.L., Benavides M.P., 2007. Endogenous salicylic acid
658 potentiates cadmium-induced oxidative stress in *Arabidopsis thaliana*. *Plant Sci.* 173, 190-197.

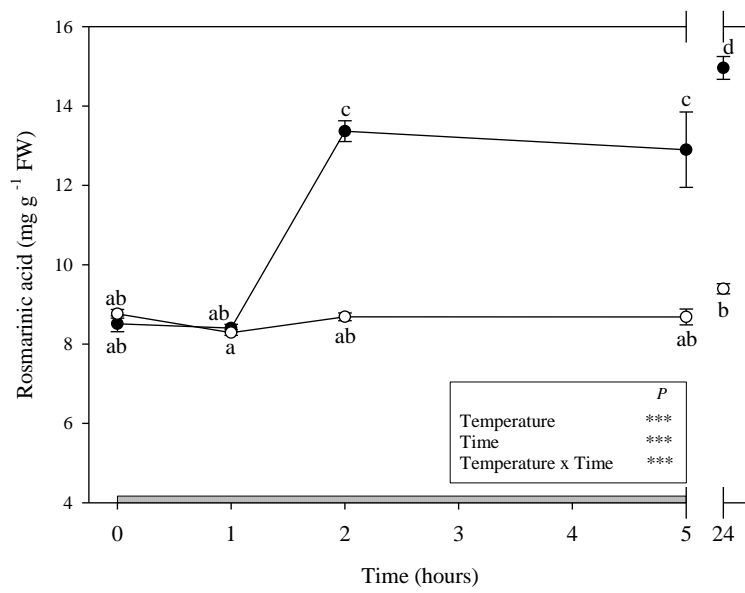
659 Zhao, Y., Yu, W., Hu, X., Shi, Y., Liu, Y., Zhong, Y., Wang, P., Deng, S., Niu, J., Yu, X., 2018.
660 Physiological and transcriptomic analysis revealed the involvement of crucial factors in heat stress
661 response of *Rhododendron hainanense*. *Gene* 660, 109-119.

662 Zhao, J.L., Zhou, L.G., Wu, J.W., 2010. Effects of biotic and abiotic elicitors on cell growth and
663 tanshinone accumulation in *Salvia miltiorrhiza* cell cultures. *Appl. Microbiol. Biotechnol.* 87, 137-
664 144.

665 Zou, M., Yuan, L., Zhu, S., Liu, S., Ge, J., Wang, C., 2016. Response of osmotic adjustment and
666 ascorbate-glutathione cycle to heat stress in a heat-sensitive and a heat-tolerant genotype of wucaï
667 (*Brassica campestris* L.). *Sci. Hortic.* 211, 87-94.

668

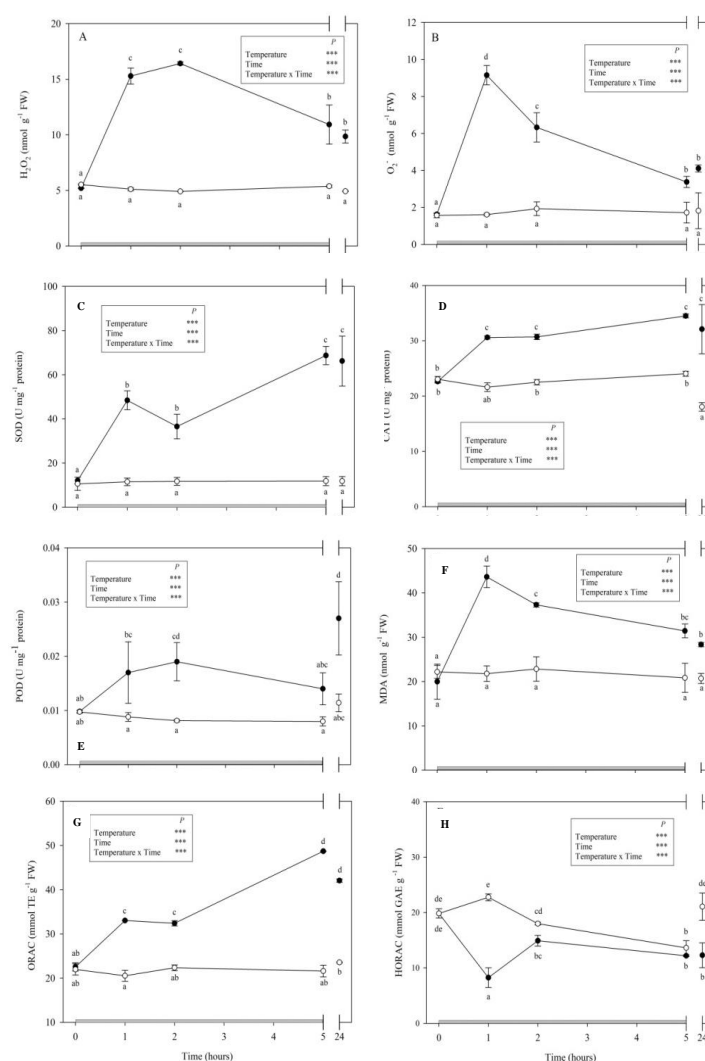
669



670

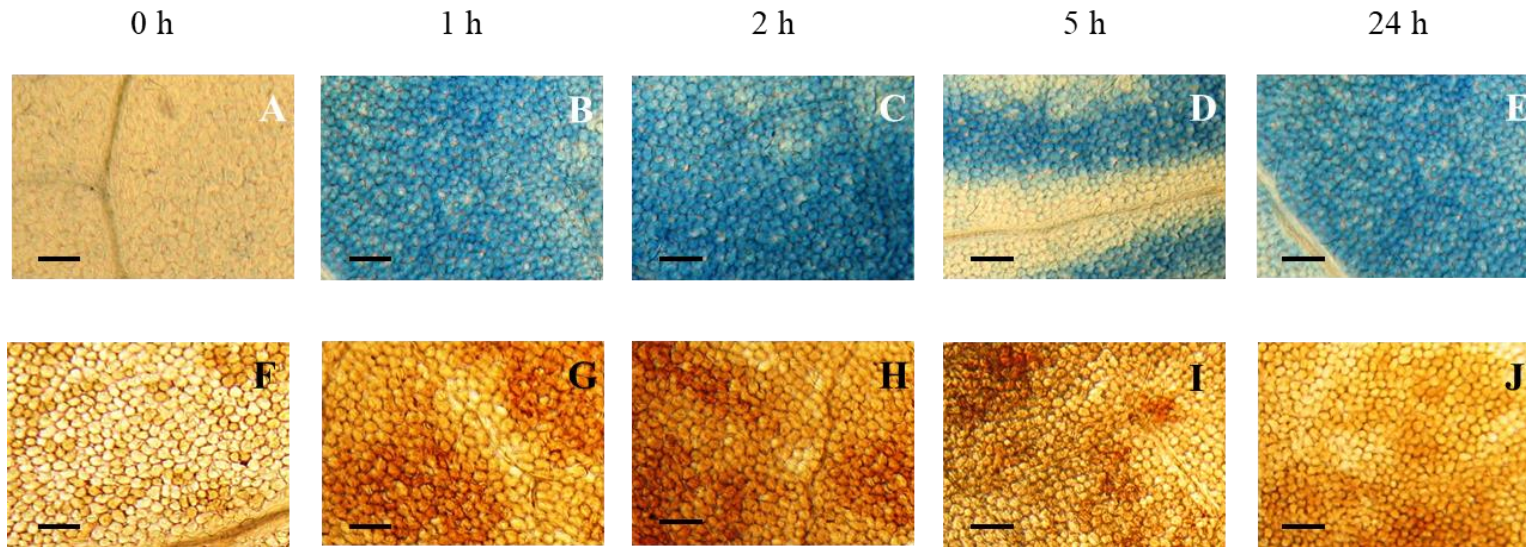
671 Fig. 1. Time course of rosmarinic acid content in leaves of *Melissa officinalis* exposed to high
 672 temperature (38°C, 5 h, closed circle) or maintained at 22°C (open circle). Data are shown as mean
 673 \pm standard error. Measurements were carried out at 0, 1, 2, 5 and 24 h from the beginning of
 674 treatment. Boxes show the results of the full-factorial two-way ANOVA with temperature and time
 675 as variability factors (***: $P \leq 0.001$). According to the Tukey's HSD Post Hoc test, different
 676 letters indicate significant differences ($P \leq 0.05$). The grey bar indicates the temperature treatment
 677 (5 h). Abbreviations: FW, fresh weight.

678



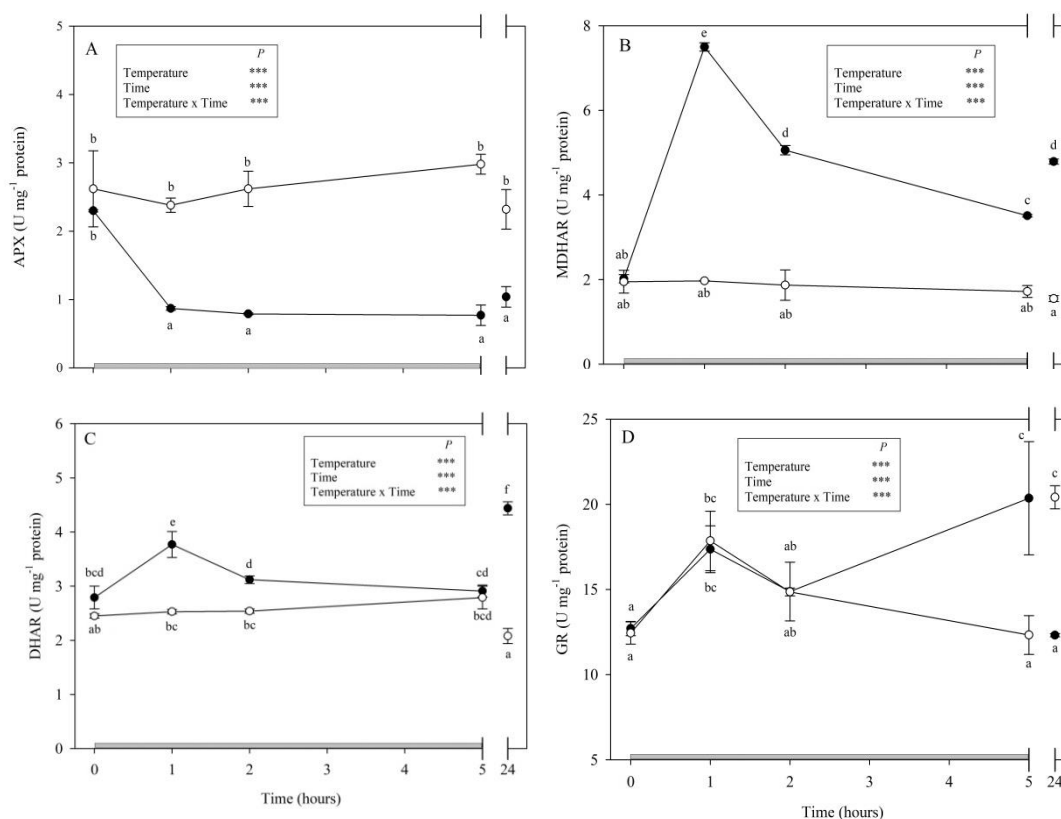
679

680 Fig. 2. Time course of hydrogen peroxide (H_2O_2 , A), superoxide anion radical ($\text{O}_2^{\bullet-}$, B), superoxide
681 dismutase activity (SOD, C), catalase (CAT, D), peroxidase (POD, E), malondialdehyde (MDA, F),
682 antioxidant capacity expressed as oxygen radical absorbance capacity (ORAC, G) and hydroxyl
683 radical antioxidant capacity (HORAC, H) in leaves of *Melissa officinalis* exposed to high
684 temperature (38°C , 5 h, closed circle) or maintained at 22°C (open circle). Data are shown as mean
685 \pm standard error. Measurements were carried out at 0, 1, 2, 5 and 24 h from the beginning of
686 treatment. Boxes show the results of the full-factorial two-way ANOVA with temperature and time
687 as variability factors (***: $P \leq 0.001$). According to the Tukey's HSD Post Hoc test, different
688 letters indicate significant differences ($P \leq 0.05$). The grey bar indicates the temperature treatment
689 (5 h). Abbreviations: FW, fresh weight; GAE, gallic acid equivalents; TE, trolox equivalents.



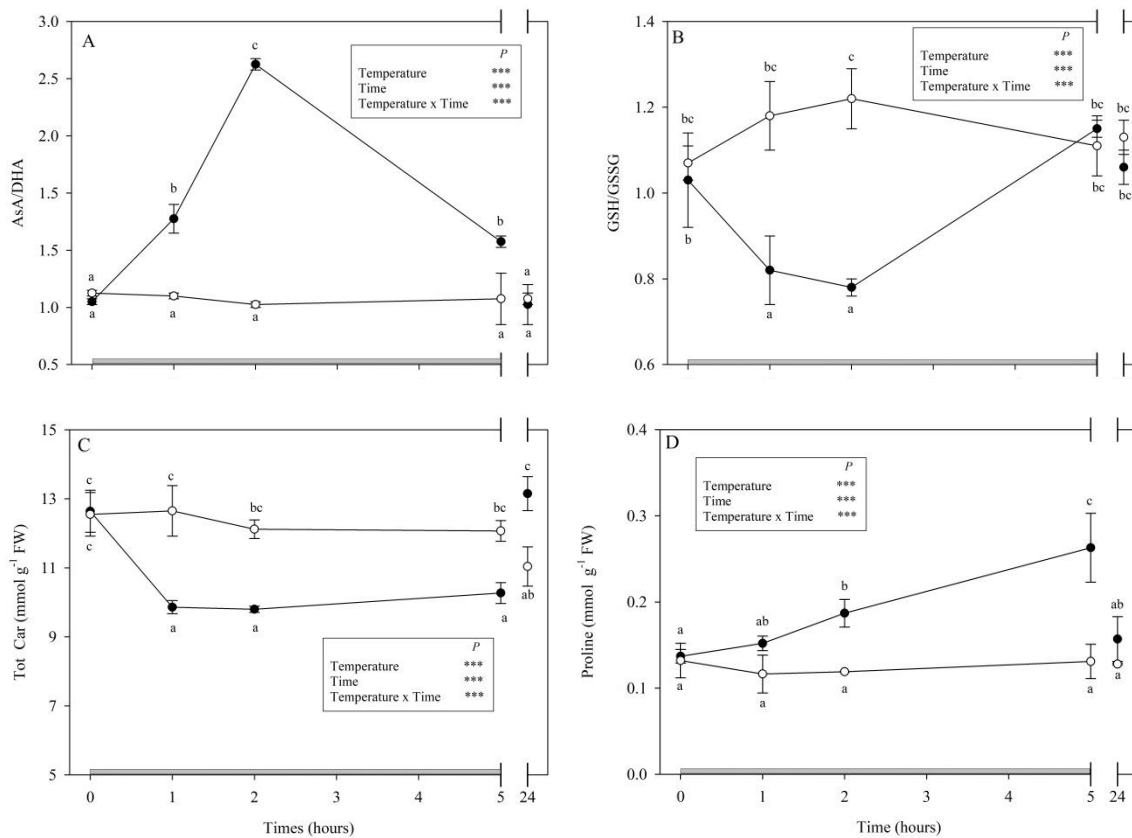
690

691 Fig. 3. Localization of dead cells visualized with Evans blue staining (A-E) and of hydrogen peroxide (H_2O_2) visualized with the 3,3'-
 692 diaminobenzidine (DAB) uptake method (F-J) in leaves of *Melissa officinalis* exposed to high temperature (38°C, 5 h). The assays were performed
 693 at 0 (i.e. before starting the treatment), 1, 2, 5 and 24 h from the beginning of treatment. Bars: 50 μm.



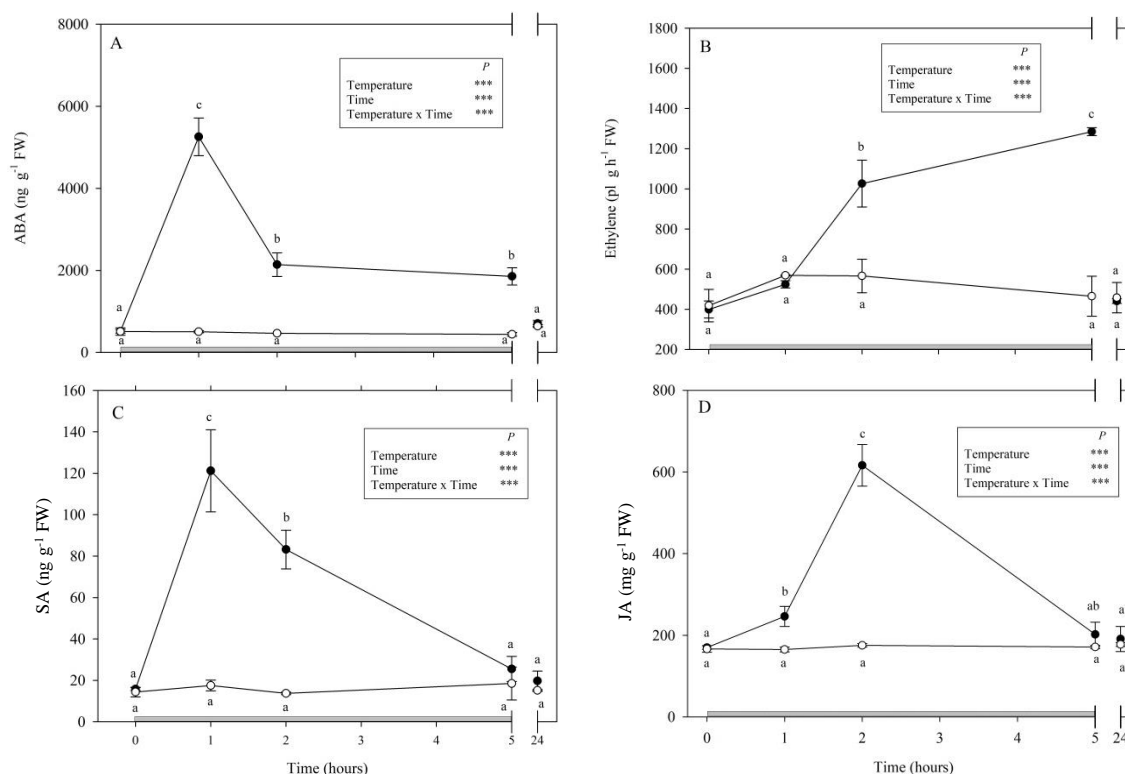
694

695 Fig. 4. Time course of ascorbate peroxidase (APX, A), monodehydroascorbate reductase (MDHAR,
696 B), dehydroascorbate reductase (DHAR, C) and glutathione reductase (GR, D) activities in leaves
697 of *Melissa officinalis* exposed to high temperature (38°C, 5 h, closed circle) or maintained at 22°C
698 (open circle). Data are shown as mean \pm standard error. Measurements were carried out at 0, 1, 2, 5
699 and 24 h from the beginning of treatment. Boxes show the results of the full-factorial two-way
700 ANOVA with temperature and time as variability factors (***: $P \leq 0.001$). According to the
701 Tukey's HSD Post Hoc test, different letters indicate significant differences ($P \leq 0.05$). The grey
702 bar indicates the temperature treatment (5 h).



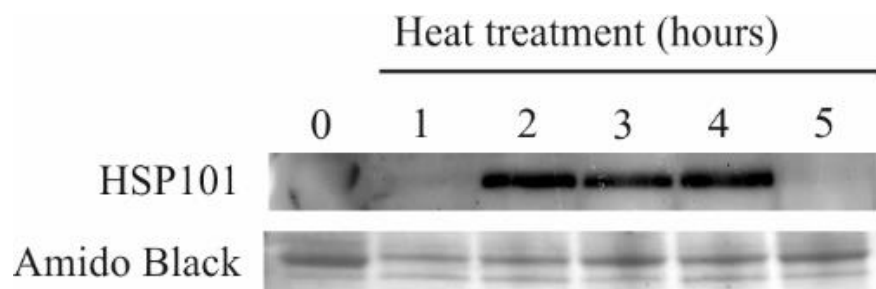
703

704 Fig. 5. Time course of reduced/oxidized ascorbate (AsA/DHA, A) and glutathione (GSH/GSSG, B)
 705 ratio, total carotenoids (Tot Car, C) and proline (D) in leaves of *Melissa officinalis* exposed to high
 706 temperature (38°C, 5 h, closed circle) or maintained at 22°C (open circle). Data are shown as mean
 707 ± standard error. The measurements were carried out at 0, 1, 2, 5 and 24 h from the beginning of
 708 treatment. Measurements were carried out at 0, 1, 2, 5 and 24 h from the beginning of treatment.
 709 Boxes show the results of the full-factorial two-way ANOVA with temperature and time as
 710 variability factors (***: $P \leq 0.001$). According to the Tukey's HSD Post Hoc test, different letters
 711 indicate significant differences ($P \leq 0.05$). The grey bar indicates the temperature treatment (5 h).
 712 Abbreviations: FW, fresh weight.



713

714 Fig. 6. Time course of abscisic acid (ABA, A) and ethylene (B), salicylic (SA, C) and jasmonic (JA,
715 D) acids content in leaves of *Melissa officinalis* exposed to high temperature (38°C, 5 h, closed
716 circle) or maintained at 22°C (open circle). Data are shown as mean \pm standard error. Measurements
717 were carried out at 0, 1, 2, 5 and 24 h from the beginning of treatment. Boxes show the results of
718 the full-factorial two-way ANOVA with temperature and time as variability factors (***: $P \leq$
719 0.001). According to the Tukey's HSD Post Hoc test, different letters indicate significant
720 differences ($P \leq 0.05$). The grey bar indicates the temperature treatment (5 h). Abbreviations: FW,
721 fresh weight.



722

723 Fig. 7. Immunoblotting of proteins extracted from hydroponic cultured of *Melissa officinalis*
 724 exposed to high temperature (38°C, 5 h). The antibodies used recognized HSP101. Blots were
 725 stained with Amido Black to confirm loading and transfer.

726 **Supplementary material**

727 *Reagents and standards*

728 2,20-azobis(2-amidinopropane) dihydrochloride (AAPH), 2,2-dipyridyl, 3'-(1-[phenylamino-
729 carbonyl]-3,4-tetrazolium)bis(4-methoxy-6-nitro) benzene-sulfonic acid hydrate (XTT), 3,30-
730 diaminobenzidine (DAB), 4,7-diphenyl-1,10-phenanthroline, 4-vinilpyridine, 5',5'-dithiobis-2-
731 nitrobenzoic acid (DTNB), 6-benzylaminopurine (BAP), β -nicotinamide adenine dinucleotide,
732 reduced disodium salt hydrate (NADH), β -nicotinamide adenine dinucleotide 2'-phosphate reduced
733 tetrasodium salt hydrate (NADPH), agar, amido black, AsA, bovine serum albumin (BSA), chloral
734 hydrate, cobalt (Co, II) fluoride tetrahydrate, cyclohexane, dehydroascorbic acid (DHA), disodium
735 hydrogen phosphate (Na_2HPO_4), dithiothreitol (DDT), ethanol, ethylacetate,
736 ethylenediaminetetraacetic acid (EDTA), ethylenediaminetetraacetic acid disodium salt dihydrate
737 (Na_2EDTA), Evans Blue, glacial acetic acid, guaiacol, hydrogen peroxide (H_2O_2), iron(III) chloride
738 (FeCl_3), methanol, N-ethylmaleimide, nitroblue tetrazolium (NBT), fluorescein (FL), gallic acid,
739 glycerol, lactic acid, magnesium chloride (MgCl_2), methionine, ninhydrin, ortho-phosphoric acid,
740 phenol, phenylmethylsulfonyl fluoride (PMSF), phosphoric acid (H_3PO_4), polyvinylpolypyrrolidone
741 (PVPP), potassium phosphate monobasic and dibasic, oxidized glutathione (GSSG), reduced
742 glutathione (GSH), glutathione reductase (GR), riboflavin, sodium acetate, sodium hypochlorite,
743 sodium phosphate monobasic and dibasic, sucrose, sulfosalicylic acid, tetrazolium dye sodium,
744 sulfosalicylic acid, thiobarbituric acid (TBA), toluene, trichloroacetic acid (TCA), triethanolamine,
745 Tris-HCl, trolox and Tween-20[®] were supplied by Sigma-Aldrich (Milan, Italy). Invitrogen
746 (Carlsbad, CA, USA) supplied Bis-Tris gel and peroxidase (POD; EC 1.11.1.7, from horseradish).
747 Standards of ethylene (ET), salicylic acid (SA) and jasmonic acid (JA) were chromatographically
748 pure and purchased from Sigma-Aldrich (Milan, Italy). EuroClone (Milan, Italy) supplied ECL
749 reagent. Antibody against Hsp101 (AS07 253, 1:1000) and horseradish POD-conjugated anti-rabbit
750 IgG (AS09 602, 1:20000) were purchased from Agrisera (Vännäs, Sweden).

751 *Plant material, culture conditions and heat treatment*

752 Mature individuals of *M. officinalis* were obtained from a commercial greenhouse placed in Central
753 Italy. Cuttings from these plants were moved in plastic pots containing a mixture of soil and peat
754 (1:1), and grown for 4 months under field conditions. Apical portions of plants (10 mm length)
755 were then submerged in 2% (v/v) Tween-20[®] for 10 min, in 70% (v/v) ethanol for 30 s, sterilized
756 with a 15% (v/v) sodium hypochlorite solution for 10 min and finally rinsed 5 times in sterile
757 distilled water. The explants were so placed on a MS medium (Murashige and Skoog, 1962)
758 supplemented with 0.5 ppm BAP, 3% (w/v) sucrose and 0.8% (w/v) agar. Shoots proliferation was
759 rapidly obtained and successive subcultures performed at 4-weekly intervals. Following culture
760 conditions and heat treatment are reported in Materials and methods.

761 *Rosmarinic acid content*

762 Rosmarinic acid content was determined following Tonelli et al. (2015), with minor modifications.
763 Plantlets (10 mg FW) were suspended in 1 ml 70 % ethanol and mixed vigorously. Extraction was
764 conducted by sonicating the samples at 70°C for 10 min twice with vigorous mixing in between.
765 After centrifugation for 10 min at 6,000 × g and 4°C, the supernatant was diluted 1:10 with 40 %
766 methanol acidified with 0.01 % H₃PO₄. After another 5 min centrifugation (same set as the previous
767 one) a HPLC analysis was performed at room temperature using a PU-2089 four-solvent low-
768 pressure gradient pump with a UV-2077 UV/Vis multichannel detector (Jasco, Easton, MD, USA)
769 and a Macherey-Nagel C18 250/4.6 Nucleosil 100-5 column equipped with a guard column, at a
770 flow rate of 1 ml min⁻¹, using acetonitrile (eluent A) and aqueous 0.1% H₃PO₄ (eluent B). The
771 gradient elution was set as follows: 0.0-0.4 min, B 95%; 0.4-0.5 min, B 95-85%; 0.5-10 min, B 85-
772 80%; 10-20 min, B 80-60%; 20-21 min, B 60-5%; 21-25 min, B 5%; 25-26 min, B 5-95%; 26-30
773 min, B 95%. The injection volume was 20 µl and the analyses were performed at room temperature.
774 Rosmarinic acid was detected at 325 nm and quantified on the basis of the integrated peak area, as
775 compared with a standard curve.

776 *ROS production, SOD activity, lipid peroxidation and antioxidant capacity*

777 Hydrogen peroxide production was estimated fluorimetrically using the Amplex Red Hydrogen
778 Peroxide/Peroxidase Assay Kit (Molecular Probes, Invitrogen, Carlsbad, CA, USA), according to
779 Shin et al. (2005). Plantlets (10 mg FW) were homogenized in a mortar with 0.4 ml of 20 mM
780 potassium-phosphate (K/P) buffer (pH 6.5) and centrifuged at $12,000 \times g$ for 20 min at 4°C. The
781 reaction mixture contained 20 mM K/P buffer (pH 6.5), 50 μ M of 10-acetyl-3,7-
782 dihydrophenoxazine, 0.1 U ml⁻¹ of POD and 50 μ l of the supernatant. Samples were incubated at
783 25°C for 30 min in the dark and the resorufin fluorescence (excitation/emission=530/590 nm) was
784 quantified with a fluorescence/absorbance microplate reader (Victor3 1420 Multilabel Counter,
785 Perkin Elmer, Waltham, MA, USA), after subtracting the background fluorescence due to the buffer
786 solution and to the assay reagents. Each result was plotted against a H₂O₂-standard curve (from 0 to
787 100 μ M). The superoxide radical (O₂^{•-}) determination was based on the reduction of XTT by O₂ to
788 a soluble XTT formazan, according to Tonelli et al. (2015). Plantlets (100 mg FW) were
789 homogenized in a mortar with 0.5 ml of 50 mM K/P buffer (pH 7.8) and centrifuged at $12,000 \times g$
790 for 20 min at 4°C. The reaction mixture contained 50 mM Tris-HCl buffer (pH 7.5), 0.5 mM XTT
791 and 50 μ l of the supernatant in a final volume of 1.5 ml. Samples were incubated at room
792 temperature for 120 min and the reduction of XTT formazan was quantified with a
793 spectrophotometer (Jenway 6505 UV-vis, Cole-Parmer, Stone, Staffordshire, UK) at 470 nm, after
794 subtracting the background absorbance due to the buffer solution and to the assay reagents. The
795 quantity of O₂^{•-} produced was determined using the molar extinction coefficient $2.16 \times 10^4 \text{ M}^{-1} \text{ cm}^{-1}$.

796 Superoxide dismutase (SOD, EC 1.15.1.1) activity was assayed according to the method of
797 Beyer and Fridovich (1987). The reaction mixture contained 50 mM K/P buffer (pH 7.0), 1.0 mM
798 EDTA, 13 mM methionine, 75 μ M NBT, 2.0 μ M riboflavin and 0-40 μ l of enzyme extract. Samples
799 were incubated for 15 min under a fluorescent lamp (11 W, Philips FCN PL 11, Milan, Italy) and

800 absorbance at 560 nm was read against unilluminated samples using a double-beam
801 spectrophotometer (Shimadzu UV-1800, Shimadzu Corporation, Milan, Italy).

802 Lipid peroxidation was determined by the thiobarbituric acid reactive substances (TBARS)
803 method (Heath and Packer, 1968). Plantlets (400 mg FW) were suspended in 1 ml 0.1% TCA (w/v)
804 and centrifuged at $12,000 \times g$ for 10 min at 4°C. 400 µl of supernatant were mixed with 1,600 µl of
805 20% TCA with 0.5 % TBA. The mixture was heated at 95°C (25 min), quickly cooled and
806 centrifuged at $12,000 \times g$ for 10 min at 4°C. The supernatant was used to determine the
807 malondialdehyde (MDA) concentration at 532 nm corrected for nonspecific turbidity by subtracting
808 the absorbance at 600 nm using a spectrophotometer (the same reported above). The amount of
809 MDA was calculated by using an extinction coefficient of $155 \text{ mM}^{-1} \text{ cm}^{-1}$.

810 The antioxidant properties were assessed spectrofluorimetrically by the Oxygen Radical
811 Absorption Capacity (ORAC) and Hydroxyl Radical Antioxidant Capacity (HORAC) assays. The
812 ORAC activity method is based on the oxidation of a fluorescent probe by peroxy radicals
813 produced by a free radical initiator, AAPH (Ou et al., 2001). The HORAC activity method is based
814 on the oxidation-mediated quenching of a fluorescent probe by hydroxyl radicals produced by a
815 hydroxyl radical initiator and Fenton reagent (Ou et al., 2002). Plantlet material (100 mg FW) was
816 added to 1 ml of 100% cold methanol and centrifuged at $12,000 \times g$ for 10 min at 4°C. 10 µl of
817 supernatant were mixed with 170 µl of 48 nM FL. The reagents were transferred into the main
818 reagent wells (OptiPlate 96 F plates, Perkin Elmer, Waltham, MA, USA) and incubated at 37°C for
819 20 min before recording the initial fluorescence (excitation/emission=485/527 nm). After
820 incubation, 20 µl of AAPH reagent (51.5 mM final concentration) were added, and fluorescence
821 readings were taken every minute for a duration of 60 min. The P buffer was used as blank, and
822 Trolox solution (0.78-25 µM) as standard. The final ORAC values were calculated by using a
823 regression equation between the Trolox concentration and the net area under the FL decay curve
824 and were expressed as Trolox equivalents (TE) as µmol per gram FW. In the HORAC assay, 10 µl

825 of extract were mixed with 170 μ l of 48 nM fluorescein (605 mM final concentration) and
826 incubated at 37°C for 10 min, before recording the initial fluorescence
827 (excitation/emission=485/520 nm). After incubation, 10 μ l of H₂O₂ (27.5 mM final concentration)
828 and 10 μ l of Co (II) (230 μ M final concentration) solutions are added subsequently, and
829 fluorescence readings were taken every minute for a duration of 60 min. The P buffer was used as
830 blank, and gallic acid solution (100-600 μ M) as standard. The final HORAC values are calculated
831 using a regression equation between the standard antioxidant concentration and the net area under
832 the curve. One HORAC unit is assigned to the net protection area provided by 1 μ M gallic acid and
833 the activity of the sample is expressed as μ mol gallic acid equivalent (GAE) per gram of FW.

834 *Cell and membrane damage*

835 For visualization of dead cells, Evans Blue staining was used according to the method of Keogh et
836 al. (1980) with slight modifications. Plantlets were boiled for 1 min in a mixture of phenol, lactic
837 acid, glycerol and distilled water containing 20 ppm Evans Blue (1:1:1:1), prepared immediately
838 before use. Plantlet material was then clarified overnight in a solution of 2.5 g l⁻¹ chloral hydrate in
839 water.

840 For determination of H₂O₂, fresh plantlet material was stained with DAB using a
841 modification of the procedure described by Thordal-Christensen et al. (1997). Fresh plantlets were
842 submerged for 8 h in a DAB solution (1 mg ml⁻¹, pH 5.6) prepared in distilled water. After that, the
843 samples were soaked in boiling 70% ethanol and clarified overnight in a solution of 2.5 g l⁻¹ chloral
844 hydrate in water. Observations were performed under a light microscope (DM 4000 B, Leica,
845 Wetzlar, Germany).

846 *Chloroplast and general enzymatic scavenging of ROS*

847 Catalase (CAT, EC 1.11.1.6) activity was assayed according to the method of Aebi (1984), by
848 monitoring the decomposition of H₂O₂ for 1 min through the decrease in absorbance at 240 nm. The

849 reaction mixture contained 50 mM K/P buffer (pH 7.0) with 8.8 mM H₂O₂ and 20 µl of enzyme
850 extract. The concentration of CAT was determined assuming an absorbance coefficient of 0.04 mM⁻¹
851 cm⁻¹. Peroxidase activity was assayed according to the method of Hemeda and Klein (1990) by
852 measuring the decomposition of H₂O₂ for 10 min through the increase in absorbance at 470 nm. The
853 reaction mixture contained 50 mM K/P buffer (pH 6.1) with 16 mM guaiacol, 0.08 mM H₂O₂ and
854 50 µl of enzyme extract. The concentration of POD was determined assuming an absorbance
855 coefficient of 26.5 mM⁻¹ cm⁻¹.

856 Ascorbate peroxidase (APX, EC 1.11.1.11) activity was assayed according to the method of
857 Nakano and Asada (1981), by measuring the oxidation of AsA at 290 nm for 1 min (at 25°C). The
858 reaction mixture contained 50 mM K/P buffer (pH 7.0), 0.4 mM AsA, 0.15 mM EDTA, 5.0 mM
859 H₂O₂ and 20 µl of enzyme extract. The concentration of APX was determined assuming an
860 absorbance coefficient of 2.8 mM⁻¹ cm⁻¹.

861 Monodehydroascorbate reductase (MDHAR, EC 1.6.5.4) activity was assayed according to
862 the method Huang et al. (2008) by measuring the oxidation of NADH for 1 min through the
863 decrease in absorbance at 340 nm. The reaction mixture contained 50 mM K/P buffer (pH 6.5),
864 0.33 mM NADH, 3 mM AsA and 20 µl of enzyme extract. The concentration of MDHAR was
865 determined assuming an absorbance coefficient of 3.3 mM⁻¹ cm⁻¹. Dehydroascorbate reductase
866 (DHAR, EC 1.8.5.1) activity was assayed, by measuring the production of AsA by DHA reduction
867 at 265 nm for 1 min (at 25°C), according to the method of Hossain and Asada (1984). The reaction
868 mixture contained 50 mM K/P buffer (pH 6.5), 1 mM GSH, 0.3 mM DHA and 50 µl of enzyme
869 extract. The concentration of DHAR was determined assuming an absorbance coefficient of 14 mM⁻¹
870 cm⁻¹. Glutathione reductase (EC 1.6.4.2) activity was assayed according to the method of Foyer
871 and Halliwell (1976) by monitoring the oxidation of NADPH by GSSG for 3 min (at 30°C) through
872 the decrease in absorbance at 340 nm. The reaction mixture contained 50 mM K/P buffer (pH 7.8),
873 0.5 mM GSSG, 0.25 mM NADPH, 0.2 mM Na₂EDTA and 50 µl of enzyme extract. The

874 concentration of GR was determined assuming an absorbance coefficient of $6.22 \text{ mM}^{-1} \text{ cm}^{-1}$. For all
875 assays, proteins were determined according to Bradford (1976), using BSA as standard.

876 *Chloroplast and general non-enzymatic scavenging of ROS*

877 Ascorbate and DHA content were measured spectrophotometrically, according to Kampfenkel et al.
878 (1995). Plantlets (250 mg FW) were homogenized in a mortar with 0.6 ml of cold 5% (w/v) TCA
879 and centrifuged at $12,000 \times g$ for 15 min at 4°C . This assay is based on the reduction of ferric ion
880 (Fe^{3+}) to ferrous ion (Fe^{2+}) with AsA in acid solution followed by formation of the red chelate
881 between Fe^{2+} and 4,7-diphenyl-1,10-phenanthroline (bathophenanthroline) that absorbs at 525 nm.
882 The AsA assay mixture 50 μl of the sample extract, 150 μl of 200 mM K/P (pH 7.4), 50 μl of 6%
883 (w/v) TCA and 50 μl of water. The total ascorbate (AsA + DHA) assay mixture contained 50 μl of
884 the sample extract, 150 μl of 200 mM K/P (pH 7.4), 50 μl of 6% (w/v) TCA and 50 μl of 10 mM
885 DTT. The reaction mixture was left standing at room temperature for 15 min and after reduction of
886 DHA to AsA, 50 μl of 0.5% (w/v) N-ethylmaleimide was added. The color was developed in both
887 assays by adding the following reagents in this sequence: 250 μl of 10% (w/v) TCA, 200 μl of 42%
888 (v/v) ortho-phosphoric acid, 200 μl of 4.0% (w/v) 2,2-dipyridyl in 70% ethanol and 100 μl of 3%
889 (v/v) FeCl_3 . The final volume was 1 ml. Controls without extract were also run and the solution was
890 allowed to stand at 30°C at room temperature for Fe^{2+} -bathophenanthroline complex to develop.
891 Dehydroascorbic acid levels were estimated on the basis of the difference between total ascorbate
892 and AsA values. A standard calibration curve covering 0-10 nM of AsA or DHA range was used.

893 Supernatants (the same reported above) were also used for total and oxidized glutathione
894 determinations by the DTNB-GSSG reductase recycling procedure, as reported in Pellegrini et al.
895 (2013). Total glutathione equivalents were determined from the reaction mixture containing 0.20 ml
896 of reagent 1 [15 mM of Na_2EDTA , 0.3 mM of DTNB and 0.04% (w/v) of BSA in K/P buffer
897 0.1mM (pH 7.2)], 0.16 ml of reagent 2 [1 mM of Na_2EDTA and 0.02% (w/v) of BSA in K/P buffer
898 0.1 mM (pH 7.2) which contained an equivalent of 1.5 U ml^{-1} of GR], 0.17 ml of 5% (w/v)

899 Na_2HPO_4 and 0.02 ml of extract. The reaction started by the addition of 0.02 ml of 0.66% (w/v)
900 NADPH in K/P buffer 0.1 mM (pH 7.2). The mixture was incubated at 30°C for 1 min and the
901 reaction was followed as the rate of change of absorbance at 412 nm for 1 min at 25°C. Oxidized
902 glutathione was determined after removal of GSH from the sample extract by derivatization with 4-
903 vinylpyridine. The extract (0.25 ml) was incubated for 60 min at 25°C with 0.004 ml of 50% (v/v) of
904 4-vinylpyridine-ethanol and 0.016 ml of 50% (v/v) of triethanolamine. Reduced glutathione was
905 determined from the reaction mixture containing 0.20 ml of reagent 1, 0.17 ml of 5% (w/v)
906 Na_2HPO_4 and 0.02 ml of extract. The amount of GSH was calculated by subtracting the GSSG
907 amount, as GSH equivalents, from the total glutathione amount. A standard calibration curve where
908 GSH equivalents (0-10 mM) were plotted against the slope of change in absorbance at 412 nm was
909 produced for determinations.

910 Proline (Pro) content was determined following Bates et al. (1973), with some minor
911 modifications. Plantlets (100 mg FW) were suspended in 1.0 ml of 3% sulfosalicylic acid. The
912 homogenates were centrifuged at $12,000 \times g$ for 5 min at 4°C. The supernatant was mixed with
913 equal volumes of glacial acetic acid (1 ml) and 1 ml of ninhydrin reagent (1.25 g ninhydrin, 30 ml
914 of glacial acetic acid and 20 ml of 6 M H_3PO_4) and incubated for 1 h at 100°C. The reaction was
915 stopped by placing the test tubes in ice-cold water. The samples were vigorously mixed with 2 ml
916 toluene. After 20 s, the light absorption of the toluene phase was estimated at 520 nm, using toluene
917 as a blank. The Pro concentration was determined using a standard curve.

918 Carotenoids were measured after extracting 30 mg of leaf tissue in 0.3 ml fluorescein of
919 100% HPLC-grade methanol overnight at 4°C in the dark. Pigments were then determined by
920 HPLC (P680 Pump, UVD170U UV-VIS detector, Dionex, Sunnyvale, CA, USA) at room
921 temperature with a reverse-phase Dionex column (Acclaim 120, C18, 5 μm particle size, 4.6 mm
922 internal diameter \times 150 mm length), according to Cotrozzi et al. (2017), with some minor
923 modifications. Samples were centrifuged for 15 min at $16,000 \times g$ at 5°C and the supernatant was

924 filtered through 0.2 μm Minisart® SRT 15 aseptic filters and immediately analyzed. The pigments
925 were eluted using 100% solvent A (acetonitrile/ methanol, 75/25, v/v) for the first 14 min to elute
926 all xanthophylls, followed by a 1.5 min linear gradient to 100% solvent B (methanol/ ethylacetate,
927 68/32, v/v), 15 min with 100% solvent B, which was pumped for 14.5 min to elute β -carotene,
928 followed by 2 min linear gradient to 100% solvent A. The flow-rate was 1 ml min⁻¹. The column
929 was allowed to re-equilibrate in 100% solvent A for 10 min before the next injection. The pigments
930 were detected by their absorbance at 445 nm. To quantify the pigment content of each sample,
931 known amounts of pure authentic standards were injected into the HPLC system and an equation,
932 correlating peak area to pigment concentration, was formulated. The data were evaluated by Dionex
933 Chromeleon software, according to the manufacturer.

934 *Salicylic and jasmonic acids*

935 Conjugated and free SA were determined according to Zawoznik et al. (2007), with minor
936 modifications. Plantlets (150 mg FW) were added to 1 ml of 90 % (v/v) methanol, vortexed and
937 sonicated for 3 min. After centrifugation at 10,000 $\times g$ for 10 min at room temperature, the
938 supernatant was transferred, and the pellet was re-extracted in 0.5 ml of 100 % (v/v) methanol,
939 following the same procedure. Supernatants from both extractions were combined and evaporated at
940 30-40°C under a vacuum. The residue was resuspended in 0.25 ml of 5% (w/v) TCA and
941 partitioned twice using 0.8 ml of a 1:1 (v/v) mixture of ethylacetate/cyclohexane. The upper phase
942 containing free SA was concentrated at 30-40°C under a vacuum and the lower aqueous phase (with
943 conjugated SA) was hydrolyzed by adding 0.3 ml 8 N HCl and incubating for 60 min at 80°C. Both
944 of the SA collected from the upper phase and recovered from the lower phase were combined and
945 dissolved in 600 μl of the mobile phase, containing 0.2 M sodium acetate buffer, pH 5.5 (90 %) and
946 methanol (10 %). HPLC separation was performed at room temperature with a Dionex column
947 described above. SA was quantified fluorometrically (RF 2000 Fluorescence Detector, Dionex,
948 USA), with excitation at 305 nm and emission at 407 nm and it was eluted using the mobile phase

949 described above. The flow rate was 0.8 ml min^{-1} . To quantify the SA content, known amounts of
950 pure standard were injected into the HPLC system and an equation, correlating peak area to SA
951 concentration, was formulated.

952 For JA extraction, plantlets (150 mg FW) were added to 3 ml methanol and incubated
953 overnight at 4°C . The extract was centrifuged at $10,000 \times g$ for 10 min at room temperature and the
954 supernatant was filtered and evaporated at room temperature under a vacuum. After adding a
955 mixture of 0.2 % (v/v) aqueous acetic acid, the supernatant was filtered and immediately analyzed
956 with HPLC using the Dionex system and column described above. JA was detected by its
957 absorbance at 210 nm. The flow rate was 1 ml min^{-1} (Kramell et al. 1999). To quantify the JA
958 content, known amounts of pure standard were injected into the HPLC system and an equation,
959 correlating peak area to JA concentration, was formulated.

960